

THE CONTRIBUTIONS OF SOIL MOISTURE AND GROUNDWATER TO NON-
RAINFALL WATER FORMATION IN THE NAMIB DESERT

Bishwodeep Adhikari

Submitted to the faculty of the University Graduate School
in partial fulfillment of the requirements
for the degree
Master of Science
in the Department of Earth Sciences,
Indiana University

August 2019

Accepted by the Graduate Faculty of Indiana University, in partial fulfillment of the requirements for the degree of Master of Science.

Master's Thesis Committee

Lixin Wang, Ph.D., Chair

Lin Li, Ph.D.

Pierre-André Jacinthe, Ph.D.

© 2019

Bishwodeep Adhikari

ACKNOWLEDGEMENT

First of all, I would like to express my deepest sense of gratitude to my advisor Professor Lixin Wang for providing me the opportunity to pursue my graduate study under his mentorship in his research group. I am fully obliged to him for his continuous support, encouragement and professional advice to kindle and formulate this research. I really value the guidance he provided me for my upcoming academic endeavors.

I would also like to thank my committee members: Professor Lin Li and Professor Pierre-André Jacinthe for their insightful comments to better the quality of my thesis and their support during my school years at IUPUI.

I cannot forget to mention Dr. Kudzai Farai Kaseke, who has been a great friend of mine since the day we first met, and also for his involvement in the data collection which was important for my thesis. I would also like to express my sincere thanks to Cathy Chouinard and Cheryl Montgomery who helped me with all the paperwork during my stay at IUPUI.

I want to thank Fognet stations, which are part of the Southern African Science Service Centre from Climate Change and Adaptive Land Management (SASSCAL) for making the fog and air temperature data available. I would also like to express my gratitude to Gobabeb Research and Training Centre for hosting me and providing necessary assistance during the fieldwork.

I want to thank all my fellow graduate students in the Department of Earth Sciences who helped me directly or indirectly during my two years at IUPUI.

Last, but not the least, I thank my family members, Kapil Prasad Adhikari, Durga Adhikari, Bishaldeep Adhikari and Sabina Dhakal Adhikari for their unconditional ever-encouraging support, motivation and love for me.

My apologies that I could not address everybody by name here, but I really want to thank everyone who has been associated with me and supported me during my graduate study in one way or another.

Bishwodeep Adhikari

THE CONTRIBUTIONS OF SOIL MOISTURE AND GROUNDWATER TO NON-
RAINFALL WATER FORMATION IN THE NAMIB DESERT

Non-rainfall waters such as fog and dew are considered as important source of water in drylands, and the knowledge of possible sources of its formation is very important to make future predictions. Prior studies have suggested the presence of radiation fog in drylands; however, its formation mechanism still remains unclear. There have been earlier studies on the effects of fog on soil moisture dynamics and groundwater recharge. On the contrary, no research has yet been conducted to understand the contribution of soil moisture and groundwater to fog formation. This study, therefore, for the first time intends to examine such possibility in a fog-dominated dryland ecosystem, the Namib Desert. The study was conducted at three sites representing two different land forms (sand dunes and gravel plains) in the Namib Desert. This thesis is divided into two parts: the first part examines evidences of fog formation through water vapor movement using field observations, and the second part simulates water vapor transport using HYDRUS-1D model. In the first part of the study, soil moisture, soil temperature and air temperature data were analyzed, and the relationships between these variables were taken as one of the key indicators for the linkage between soil water and fog formation. The analysis showed that increase in soil moisture generally corresponds to similar increase in air or soil temperature near the soil surface, which implied that variation in soil moisture might be the result of water vapor movement (evaporated soil moisture or groundwater) from lower depths to the soil surface. In the second part of the study, surface fluxes of water vapor were simulated using the HYDRUS-1D model to explore whether the available surface flux was sufficient

to support fog formation. The actual surface flux and cumulative evaporation obtained from the model showed positive surface fluxes of water vapor. Based on the field observations and the HYDRUS-1D model results, it can be concluded that water vapor from soil layers and groundwater is transported through the vadose zone to the surface and this water vapor likely contributes to the formation of non-rainfall waters in fog-dominated drylands, like the Namib Desert.

Lixin Wang, Ph.D., Chair

TABLE OF CONTENTS

LIST OF TABLES	x
LIST OF FIGURES	xi
CHAPTER 1: INTRODUCTION	1
CHAPTER 2: MATERIALS AND METHODS	6
2.1 Site description	6
2.2 Data collection.....	7
2.3 Analysis of field data.....	8
2.4 HYDRUS modeling	9
2.4.1 Model description.....	9
2.4.2 Model setup	10
2.4.3 Soil hydraulic and heat transport parameters	12
2.4.4 Initial and boundary conditions	13
CHAPTER 3: RESULTS	15
3.1 Statistics of water content, fog and temperature	15
3.2 Relationship between fog, volumetric water content and temperature ...	16
3.3 HYDRUS-1D Modeling.....	18
CHAPTER 4: DISCUSSION.....	20
4.1 Field observations	20
4.2 Modeled water vapor surface fluxes	23
CHAPTER 5: CONCLUSIONS.....	26
TABLES.....	27
FIGURES.....	31

APPENDICES	45
<i>Appendix A: Volumetric water content, rainfall and fog patterns at gravel plains and sand dunes</i>	45
<i>Appendix B: Volumetric water content, soil temperature and air temperature patterns at gravel plains and sand dunes</i>	50
REFERENCES	55
CURRICULUM VITAE	

LIST OF TABLES

Table 1. Soil hydraulic parameters used in the HYDRUS-1D model for three sites: sand dunes, gravel plains, and gravel plains with groundwater presence (Gravel plains (GW)).	27
Table 2. Heat transport parameters used in the HYDRUS-1D model for three sites: sand dunes, gravel plains, and gravel plains with groundwater presence (Gravel plains (GW)).	28
Table 3. Descriptive statistics of volumetric water content from field observations for the overall study period and the 80 non-rainfall days at sand dunes and gravel plains.	29
Table 4. Statistics of volumetric water content, rainfall and fog for different hydrologic years at sand dunes and gravel plains.	30

LIST OF FIGURES

Figure 1. Extent of the Namib Desert and study site locations.....	31
Figure 2. Variation of different variables (soil temperature, air temperature, volumetric water content, fog and rain) at sand dunes from August 5, 2015 to May 22, 2018.....	32
Figure 3. Variation of different variables (soil temperature, air temperature, volumetric water content, fog and rain) at gravel plains from December 29, 2013 to June 24, 2018.	33
Figure 4. Relationship of volumetric water content with soil temperature at sand dunes from August 5, 2015 to May 22, 2018.	34
Figure 5. Relationship of volumetric water content with air temperature at sand dunes from August 5, 2015 to May 22, 2018.	35
Figure 6. Relationship of volumetric water content with soil temperature at gravel plains from December 29, 2013 to June 24, 2018.	36
Figure 7. Relationship of volumetric water content with air temperature at gravel plains from December 29, 2013 to June 24, 2018.	37
Figure 8. Relationship of volumetric water content with soil temperature at sand dunes for 80 non-rainfall days from August 19, 2015 to November 06, 2015.....	38
Figure 9. Relationship of volumetric water content with air temperature at sand dunes for 80 non-rainfall days from August 19, 2015 to November 06, 2015.....	39
Figure 10. Relationship of volumetric water content with soil temperature at gravel plains from August 19, 2015 to November 06, 2015.....	40

Figure 11. Relationship of volumetric water content with air temperature at gravel plains from August 19, 2015 to November 06, 2015.....	41
Figure 12. Observed and simulated volumetric water content at sand dunes.....	42
Figure 13. Observed and simulated volumetric water content at gravel plains.....	43
Figure 14. Actual surface flux (mm/day) obtained from HYDRUS-1D model at sand dunes, gravel plains, and gravel plains with groundwater presence (Gravel plains_GW).....	44

CHAPTER 1: INTRODUCTION

Drylands are regions where precipitation is comparatively less than potential evapotranspiration. The aridity index (AI), quantitatively defined as the ratio of precipitation to potential evapotranspiration, must be less than 0.65 for an area to be considered as drylands. Drylands can be classified using this aridity index into four sub-types: dry sub-humid lands, semi-arid lands, arid lands, and hyper-arid lands (Adeel et al., 2005; Wang et al., 2012). Drylands cover approximately 40% of the land surface and support more than 2 billion population worldwide (Wang et al., 2012).

Since water resources are severely limited in drylands, water availability poses the primary control over biological processes. Non-rainfall waters such as dew and fog, although in small amount, play an important supporting role in supplying water that is essential to maintain ecological functions in drylands (Wang et al., 2017). In arid drylands, where rainfall is sparse, fog can be the most important form of water input which could be utilized for the dryland ecosystem to increase productivity (Kaseke et al., 2017). It can also constitute a major portion of the overall hydrological input especially in some of the coastal areas which often receive very little or no rainfall in a year (Dawson, 1998). Dew formation and early morning evaporation are also important processes affecting the water balance of the upper soil layer in drylands (Zhang et al., 2009; McHugh et al., 2015).

In areas where rainfall is an inadequate source of freshwater and groundwater is depleting with time, like in some drylands, fog water collection has gained greater importance (Klemm et al., 2012). In arid drylands such as the Namib desert (west coast of Namibia in southern Africa), fog is a practical source of water which could improve the conventional sources of water in rural communities and possibly also in water supply

programs in urban areas. Fog is consumed as one of the sources of drinking water in many portions across the globe (Shanyengana et al., 2002; Kaseke and Wang, 2018). According to Prada et al. (2009), fog water is a source of groundwater recharge and an important hydrological input, which can play a vital role in the water balance. Although often neglected, Ingraham and Matthews (1988) found that fog drips can contribute to deep infiltration and groundwater recharge in arid environments. Until now, there has been multiple studies indicating the importance of fog to groundwater recharge (Ingraham and Matthews, 1988, 1995; Prada et al., 2009; Sawaske and Freyberg, 2015). Conversely, little or almost no prior research has investigated the contribution of groundwater and soil moisture to the formation of fog in the atmosphere.

In general, there are seven types of fog, four of which are based on process and place of formation (radiation fog, sea fog, steam fog and advection fog), and the remaining three are designated based on their place of occurrence irrespective of the process of their formation (coastal fog, valley fog and mountain fog) (Eugster, 2008). Out of these seven different types of fog, most studies have focused on two types, namely (i) radiation fog, which is formed mainly by a cooling mechanism, especially nocturnal cooling over the continental surface, and (ii) advection fog, which is formed because of the humidification near coastal areas or over the sea (Bergot and Guedalia, 1994).

Even though the non-rainfall waters (fog, dew and vapor) provide significant amount of water for dryland environments, these are the least studied components of the hydrological cycle. Fog and dew are originated from dissimilar meteorological phenomena. However, the majority of ecological studies have considered these inputs as one since they are not suitably characterized (Kaseke et al., 2017). Having multiple origins, non-rainfall

waters in drylands can also originate from recycling of groundwater via evapotranspiration and redistribution of water vapor in the upper soil layers. More than 50% of the total fog events in the Namib Desert were found to be non-ocean-derived or locally-generated (Kaseke et al., 2017). This suggests that this desert's fog zone is potentially shifting from advection-dominated fog to radiation-dominated fog. This highlights the urgency of studies to determine the quantity and origin of non-rainfall waters in dryland ecosystems where rainfall is expected to decline due to climate change in coming years (Kaseke et al., 2017).

Soil moisture is considered as a critical component of earth system and plays an important role in land-atmosphere interactions (Eltahir, 1998). It can be used to understand the relationship of climate, soil and vegetation in dryland ecosystems (Li et al., 2016). In water-limited dryland ecosystems, various eco-hydrological processes are dependent on soil water availability. Many factors like precipitation, evaporation, liquid water and water vapor flow influence soil moisture near the surface in drylands, and most of these factors are strongly connected. In the Namib Desert, the first millimeters of surface soil might receive enough soil moisture from non-rainfall waters like fog droplets and dew formation. Since soil water content near the soil surface in drylands is often extremely low, water vapor transport plays a critical role in the overall water flux and availability (D'Odorico and Porporato, 2006; Saito et al., 2006).

The movement of soil moisture and heat are coupled. The simultaneous movement of heat, liquid water and water vapor at the land-atmosphere interface is very significant for a range of biological phenomena, as well as water and energy balance of terrestrial ecosystems (Cahill and Parlange, 1998; Saito et al., 2006; Bittelli et al., 2008). Understanding the coupled soil heat and water transport aids in countless agricultural and

engineering uses in drylands from achieving efficient and optimum water management for crop production to assessment of leachate volume from the landfills (Khire et al., 1997; Wuest et al., 1999). The total heat flux of soil is a result of simple conduction as well as the movement of water in both the liquid and vapor states. The net soil moisture movement between any two locations can be mainly attributed to the movement of moisture in soil from one location to another caused by evaporation and subsequent recondensation. During this process of evaporation and recondensation, a significant amount of energy is transported by the water vapor since water has high latent energy of vaporization (Cahill and Parlange, 1998; Saito et al., 2006).

Non-rainfall waters and soil moisture/groundwater impact each other. Fog and dew increase soil moisture, and sometimes fog infiltrates further down to recharge groundwater systems. At the same time, soil water and groundwater could contribute to fog and dew formation. For example, using oxygen and hydrogen isotopes, a recent study confirmed that groundwater is a source of radiation fog in the Namib Desert (Kaseke et al., 2017). This determination is possible based on our knowledge of processes such as soil water evaporation, and this information is very important for our understanding of water exchange between the soil and the atmosphere (Sakai et al., 2011). Studies conducted by Sakai et al. (2011), Bittelli et al. (2008), Saito et al. (2006) and Cahill and Parlange (1998) have demonstrated that soil water can be transported up to the soil surface by evaporation. Since the amount of water as soil moisture is much smaller compared to the groundwater, it was expected that groundwater could also be transported to the surface by similar phenomenon. Furthermore, the transported soil water and groundwater to the surface can be evaporated into atmosphere contributing to the formation of non-rainfall waters.

Most past studies have explored the impact of non-rainfall waters like fog to groundwater recharge or soil moisture content. Furthermore, prior studies have suggested the prevalence of radiation fog in addition to the advection fog in the Namib Desert. The studies identified groundwater and soil moisture as possible origins for the radiation fog in the Namib Desert, but transport and formation mechanisms still remain unclear. This research hence for the first time aims to investigate the contribution of groundwater and soil moisture to the formation of radiation fog in the Namib Desert. The hypothesis of the study is that soil moisture and groundwater contribute to the formation of non-rainfall waters such as fog and dew in the fog-dominated dryland, Namib Desert. To determine the validity of that hypothesis, the research reported in this thesis document was conducted to explore relationships between volumetric soil water content, soil and air temperature, and fog occurrence in the study area. In addition, a hydrological model (HYDRUS-1D) was applied to simulate water vapor transport in the vadose zone to further evaluate the research hypothesis.

CHAPTER 2: MATERIALS AND METHODS

2.1 Site description

The Namib Desert was chosen for the study because it is a fog-dominated dryland. It is located in the coastal area of Namibia and extends from the Olifants River in South Africa to Carunjamba River in Angola, and has an overall stretch of 1,900 km along the coast of the Atlantic Ocean (Li et al., 2016). There is a wide distribution of precipitation in the Namib Desert with an annual average of 5-18 mm in the central Namib Desert, less than 50 mm along the Angolan coast in the north, and 50 -100 mm in the far south. Out of the three main land forms found in the Namib Desert, endless sand dunes cover most of the southern area which is known as the Namib “Sand Sea”, and gravel plains dominate the Central Namib Desert dotted with inselbergs of granite and limestone (Bristow et al., 2007; Li et al., 2016). Moving towards the north, the sand dunes decrease in size whereas the gravel plains prevail, and finally further north the gravel plains give way to rugged mountains and dune fields (Bristow et al., 2007; Eckardt et al., 2013; Li et al., 2016).

Two land forms, the gravel plains and the sand dunes at Gobabeb located in the Namib Desert, were selected since they share similar meteorological conditions but different soil textures. Furthermore, two sites within the gravel plains were considered in this study, one which is near the Kuiseb River with groundwater depth being about 4.5 m while another is located north to the river without groundwater influence since it is far from the river channel.

The study sites were located within the vicinity of the Gobabeb Research and Training Centre (lat. -23.55°, long. 15.04°, and elv. 405 m.a.s.l.), which is in the Central Namib Desert and about 60 km inland from the Atlantic Ocean (Figure 1). The Gobabeb

Centre is surrounded by three main land forms: gravel plains to the north and east (91% sand, 0.6% clay and 8.4% silt), sand dune sea to the west and south (74.8% sand, 5.5% clay and 19.7% silt), and the ephemeral Kuiseb River (91.5% sand, 2.1% clay, 6.4% silt) to the south of the Centre which separates the gravel plains and sand dune sea (Kaseke, 2009, 2018). The climate at Gobabeb is hyper-arid with extremely infrequent precipitation events and a mean annual precipitation of 27 mm. The mean monthly temperature at Gobabeb ranges from 17 to 24.2°C, and has an average relative humidity of around 50%, with 94 mean annual foggy days (Eckardt et al., 2013; Li et al., 2018).

2.2 Data collection

The volumetric water content and soil temperature data used in the study were collected from two sites at Gobabeb in the Namib Desert; the gravel plains and the sand dunes. The daily precipitation data were collected using the tipping-bucket setting at the gravel plains and the same data were used for the sand dunes as well because of their close proximity. The volumetric water content and soil temperature data were measured hourly at both sites using the CS655 Water Content Reflectometer (Campbell Scientific, Inc. Logan, Utah, USA). The soil probes were located at an approximate depth of 4 cm at both sites. These soil moisture probes were installed horizontally at the sites and can detect volumetric water content from 0 to 100% (with M4 command) with a high precision (<0.05%). Various meteorological data such as humidity, wind speed, wind direction and air temperature and fog were obtained from weather and Fognet stations, which are part of the Southern African Science Service Centre from Climate Change and Adaptive Land Management (SASSCAL). For the gravel plains, volumetric water content and soil

temperature data from December 29, 2013 to June 24, 2018, and for the sand dunes, data from August 5, 2015 to May 22, 2018 were used in the analysis.

Furthermore, soil moisture and soil temperature data used by Entekhabi et al. (2001) to evaluate relationship between surface temperature and soil moisture in southern Africa was retrieved and digitized to compare results of their study to those of the present research. The study by Entekhabi et al. (2001) was used to compare the results since the site considered in their study had a semi-arid environment and received a higher amount of rainfall as compared to the present research. In addition, that study represented general relationship between soil moisture and soil temperature, which would exist in most of the places with wetter climatic conditions.

2.3 Analysis of field data

Hourly volumetric water content and soil temperature were averaged while precipitation and fog data were added to obtain the daily values for analysis. In order to demonstrate the relationship of volumetric water content with soil and air temperature, simple scatter plot and box plots were used. Since relationships were found between volumetric soil water content with different variables such as soil temperature, air temperature, fog and precipitation, data were analyzed to determine how the change in volumetric water content can be explained by change in different variables. The near surface soil temperature and air temperature were used for the study to further examine if the soil temperature follows the air temperature trend. In addition, the study used soil as well as air temperature and volumetric soil water content to assess relationships, if any, between these variables. Fog and precipitation data were used to understand how the volumetric soil water content behaves with their occurrences or vice versa. The data were

analyzed for two time steps: (i) overall data available and (ii) data from August 19, 2015 to November 6, 2015 during which there was no rainfall event, in order to examine whether the relationship varies when rainfall events are considered and during periods with no rainfall events. The 80 non-rainfall days (August 19, 2015 to November 6, 2015) were chosen mainly because there were no data missing within that period, there were several fog events during that period, and this period was the one previously used by Li et al. (2018) to examine the effects of fog on soil moisture dynamics in the Namib Desert. Furthermore, the statistical analysis of data was done based on hydrologic year (October to September) since rainfall events at Gobabeb are very rare, but if these events occur, they are mostly concentrated between October and April. The rainfall seasonal distribution at the study sites is similar to Windhoek where the rainfall is very seasonal and concentrated within the above mentioned months (Kaseke et al., 2018).

2.4 HYDRUS modeling

2.4.1 Model description

HYDRUS-1D model is often used for the simulation of one-dimensional water flow, heat movement and solute transport in variably saturated porous media (Šimůnek et al., 2013). In the present study, version 4.17 of this model was used for the simulation of water vapor transport from groundwater and soil moisture to the soil surface. The basic equation HYDRUS-1D model uses for the water flow is Richard's equation.

$$\frac{\partial \theta}{\partial t} = \frac{\partial}{\partial x} \left[K \left(\frac{\partial h}{\partial x} + \cos \alpha \right) \right] - S \quad (2.1)$$

where θ is the volumetric water content, t is time, x is the spatial coordinate considering upward direction as positive, K is the unsaturated hydraulic conductivity, h is

the water pressure head, α is the angle between the flow direction and vertical axis, and S is the sink term (see HYDRUS-1D User Manual by Šimůnek et al. (2013)).

However, since Richard's equation considers only liquid flow and ignores vapor flow, HYDRUS-1D model uses the following non-isothermal liquid and vapor flow equation (Saito et al., 2006) for the water vapor transport modeling.

$$\frac{\partial \theta_T(h)}{\partial t} = \frac{\partial}{\partial x} \left[(K + K_{vh}) \left(\frac{\partial h}{\partial x} + \cos \alpha \right) + (K_{LT} + K_{vT}) \frac{\partial T}{\partial x} \right] - S(h) \quad (2.2)$$

where θ_T is the total volumetric water content, T is temperature in Kelvin, K is the isothermal hydraulic conductivity of the liquid phase, K_{LT} is the thermal hydraulic conductivity of the liquid phase, K_{vh} is the isothermal vapor hydraulic conductivity, and K_{vT} is the thermal vapor hydraulic conductivity (see HYDRUS-1D User Manual by Šimůnek et al. (2013)).

2.4.2 Model setup

HYDRUS-1D model was used to simulate water vapor flow and heat transport in the vertical direction. Horizontal water transport was not considered. The soil column was considered to be homogeneous along the depth (e.g., soil was regarded as a single layer for the simulation). The iteration criteria were set to default as provided by the model. The hydraulic sub-model within HYDRUS-1D used for this study is Van Genuchten-Mualem model (Van Genuchten, 1980). Since the simulated study sites have very low vegetation cover, plant transpiration was neglected and only evaporation was considered for this study. The inverse solution option available in HYDRUS-1D was used in order to optimize the soil hydraulic parameters, α (inverse of the air-entry value) and n (pore-size distribution index) which are the coefficients of soil water retention function (see HYDRUS-1D User Manual, Šimůnek et al. (2013)). The domain of the model was

discretized into 100 number of nodes in the case of the sand dune site and the gravel plain site where no groundwater is available. However, the domain was discretized into 400 number of nodes at the gravel plain site near the river where groundwater is available at an average depth of 4.5 m.

The simulations were validated using the measured volumetric soil water content at a depth of 4 cm at the sand dunes and the gravel plains without groundwater access, while it was validated at the gravel plains having groundwater presence with an assumption that the water content here will be considerably higher than the gravel plains without groundwater. The validation period was considered after a certain duration of the model run in order to provide sufficient model spin-up time. The validation was done after 40 days at the sand dunes site since only 93 days were run in the model, and the simulation results was obtained for 53 days. However, the model spin-up period provided at the gravel plains was approximately 50% of the overall time period selected for the model run since data for 129 days were used for the model run, and 65 days would still be left for the results. The model was run for the rainless period to examine if the soil moisture and groundwater will have sufficient surface flux and evaporation for the formation of non-rainfall water at the sites. The actual surface flux obtained from the model inform what actually happens at the surface, whether the soil water evaporates or infiltrates (e.g., fraction of water moves downward). The higher amount of evaporation obtained from the model would suggest more soil water transported to the atmosphere, while higher amount of infiltration would suggest less soil water transported to the atmosphere.

2.4.3 Soil hydraulic and heat transport parameters

The soil hydraulic parameters required for the simulation of HYDRUS-1D are residual water content (Q_r), saturated water content (Q_s), saturated hydraulic conductivity (K_s), parameter α in the soil water retention function ($Alpha$), parameter n in the soil water retention function (n), and tortuosity parameter in the conductivity function (l). All these parameters except $Alpha$ and n were kept constant throughout the simulation and were obtained by the neural network prediction function (Rosetta Lite v. 1.1, (Schaap et al., 2001)) available in the HYDRUS-1D model by providing the percentage of sand, silt and clay of the soils. For this study, the percentage of sand, silt and clay for the sand dunes were 74.8, 19.7 and 5.5%, for the gravel plains without groundwater were 91, 8.4 and 0.6%, and for the gravel plains near river with groundwater availability were 91.5, 6.4 and 2.1%, respectively. The parameter $Alpha$ and n were optimized during the calibration by inverse modeling (available in HYDRUS-1D model) of daily observed volumetric water contents of the soil at selected depths and locations. The soil hydraulic parameters used for the study are presented in Table 1.

The heat transport parameters for the model are volume fraction of solid phase and organic matter, longitudinal thermal dispersivity, coefficient b_1 , b_2 and b_3 for thermal conductivity function, and volumetric heat capacities of solid phase (C_n), organic matter (C_o) and liquid phase (C_w). The default values of coefficients for thermal conductivity function and volumetric heat capacities as provided by the HYDRUS-1D model are used for all sites, and the thermal conductivity equation provided by Chung and Horton (1987) was used for the heat transport process. The heat transport parameters used in the study are presented in Table 2.

2.4.4 Initial and boundary conditions

In order to solve the Richard's equation for water flow, the initial distribution of pressure head or water content within the flow domain is required. In this study, the initial condition is provided in terms of water content as:

$$\theta(x, t) = \theta_i(x) \quad , \quad t = t_0 \quad (2.3)$$

where $\theta_i[L]$ is defined as a water content function of x , and t_0 is the time when the simulation starts (see HYDRUS-1D User Manual, Šimůnek et al. (2013)). Since the daily variation of water content was used for the simulation in this study, the water content and temperature values prior to the day selected as first day of simulation were set as initial quantities.

The atmospheric boundary conditions with surface layer were selected for the water flow at the upper boundary. Precipitation, potential evapotranspiration, minimum allowed pressure head at the soil surface that facilitate evaporation, and time-dependent temperature of the soil surface were supplied into the model at a daily temporal resolution as time variable boundary conditions at upper boundary. The average evaporation of 0.65 mm/day at the gravel plains (Li et al., 2018) was used for the simulation period at all sites because of their close proximity, and the plant transpiration was neglected since there were very low vegetation cover around the sites. At the lower boundary, variable flux condition was used at the sand dunes and the gravel plains without groundwater since soil moisture will change with time due to the evaporation, and flux will not be temporally constant. However, at the gravel plains near river with groundwater access, the lower boundary condition is set to be constant water content since soil is likely saturated near the soil-

groundwater boundary. The time dependent temperature of soil at the surface and lower boundary was considered as the boundary conditions for the heat transport process.

CHAPTER 3: RESULTS

3.1 Statistics of water content, fog and temperature

The mean volumetric water content for the study period at the sand dunes and the gravel plains were found to be 0.771% and 2.105%, respectively (Table 3). The descriptive statistics for the mean volumetric water content for the entire study period at the sand dunes was explained by the Kurtosis (K-value) of 34.82 along with the skewness of 4.95 (Table 3). For the gravel plains, the K-value was found to be 18.52 with the skewness of 3.90 during the entire study period (Table 3). The average volumetric water content at the sand dunes and the gravel plains for the 80 non-rainfall days from August 19, 2015 to November 06, 2015 was found to be 0.639% and 1.499%, respectively (Table 3). For the 80 non-rainfall period, the K-value and skewness were 0.47 and -0.54, respectively at the sand dunes, and were 1.20 and 0.73, respectively at the gravel plains (Table 3). These indicated that the volumetric water content was normally distributed around their respective means for the 80 non-rainfall days while it deviated from normality for the entire study period at both sites (Table 3). The volumetric water content at both sites seemed to have nearly daily fluctuations with few distinct peaks within the study period (Figure 2 and 3). There were few rainfall events but whenever there was a rainfall event, the volumetric water content reached a peak which descended gradually over a time. Some times during the descending phases, there were various fog events (Figure 2 and 3).

The average annual rainfall at the study site was only 7.6 ± 8.88 mm based on five hydrologic years. The rainfall in the 2017-2018 hydrologic year was extremely high (23 mm), while it remained below 10 mm for the remaining four hydrologic years. There were only 18 rainfall days during the five hydrologic years considered in the study. The average

annual fog at the site was 132.79 mm with 184 fog days during three hydrologic years (two years' fog data not available, Table 4). There was 24 fog days during the 80 non-rainfall period from August 19, 2015 to November 06, 2015. The average water content was $2.13 \pm 0.5\%$ for the five hydrologic years at the gravel plains and was $0.76 \pm 0.2\%$ for four hydrologic years at the sand dunes (one year data not available, Table 4). When the abnormal hydrologic year (2017-2018) with very high rainfall was removed, the average water content was $1.94 \pm 0.1\%$ for the gravel plains and was $0.66 \pm 0.1\%$ for the sand dunes (Table 4).

The mean soil temperature and air temperature at both sites displayed similar trends. At the sand dunes, the mean soil temperature during the entire study period was $24.09\text{ }^{\circ}\text{C}$, and was $25.30\text{ }^{\circ}\text{C}$ for the 80 non-rainfall period. Similarly, at the gravel plains, the mean soil temperature was $25.78\text{ }^{\circ}\text{C}$ for the entire study period and $23.48\text{ }^{\circ}\text{C}$ for the 80 non-rainfall period. The soil temperature varied from $16.09\text{ }^{\circ}\text{C}$ to $39.73\text{ }^{\circ}\text{C}$ for the entire study period and from $16.66\text{ }^{\circ}\text{C}$ to $32.38\text{ }^{\circ}\text{C}$ for the 80 non-rainfall period at the sand dunes, while it varied from $14.33\text{ }^{\circ}\text{C}$ to $37.41\text{ }^{\circ}\text{C}$ for the entire study period and from $16.07\text{ }^{\circ}\text{C}$ to $31.09\text{ }^{\circ}\text{C}$ for the 80 non-rainfall period at the gravel plains. Similarly, the air temperature ranged from $9.47\text{ }^{\circ}\text{C}$ to $33.63\text{ }^{\circ}\text{C}$ for the entire study period at the sand dunes and from $9.41\text{ }^{\circ}\text{C}$ to $33.63\text{ }^{\circ}\text{C}$ at the gravel plains, and from $11.84\text{ }^{\circ}\text{C}$ to $27.46\text{ }^{\circ}\text{C}$ for the 80 non-rainfall period at both sites.

3.2 Relationship between fog, volumetric water content and temperature

The soil and air temperature were analogous to each other. Soil temperature increased with increase in air temperature, and vice versa (Figures 2 and 3). The soil temperature was generally found to be higher than the air temperature. The soil and air

temperature were divided into distinct 5°C bins for analyzing the relationship with volumetric water content.

The analysis of soil temperature and volumetric water content at the sand dunes showed an increase in soil water content with increase in soil temperature (Figure 4). The results were similar between the entire study period and during the 80 non-rainfall period (Figure 4 and 8). Despite of the greater number of outliers when the overall study period was considered (as compared to the 80 non-rainfall days), the relationship was not substantially affected. Likewise, the relationship between these variables showed similar characteristics at the gravel plains with an exception for soil temperatures below 15°C, i.e., the water content at soil temperature less than 15 °C was slightly higher as compared to the higher soil temperature groups. The relationship of water content with soil temperature was more pronounced and stronger at the sand dunes as compared to the gravel plains.

Similarly, the relationship of volumetric soil water content with air temperature was analyzed separately at both sites. At the sand dunes, this displayed a parallel pattern to the soil temperature and water content relationship. However, at the gravel plains, the relationship of soil water content was more noticeable with the air temperature as compared to the soil temperature. The outliers in the case of air temperature were more in the entire period than the non-rainfall days, similar to the soil temperature and water content relationship. Soil water content increased with the increase in air temperature for the entire study period as well as the 80 non-rainfall days at both sites. Overall, the volumetric soil water content increased with increase in soil and air temperature at both sites, regardless whether the entire study period with rainfall events or the 80 rainless days was considered (Figure 4 to 11).

Whenever there was a fog or rainfall event, the volumetric water content increased and reached a peak (Figure 2 and 3). However, it was also evident that as the volumetric water content declined, there were quite a few occurrences of fog events (Figure 2 and 3).

3.3 HYDRUS-1D Modeling

The HYDRUS-1D model was used to simulate the water vapor fluxes by comparing the volumetric soil water content available at the sites with model output. At the sand dunes, the model was run from August 6, 2015 to November 6, 2015 with data on August 05, 2015 provided as the initial conditions. Even though the model was run from Aug. 6, 2015, the water content obtained from the model were compared with the observed values only after 40 days (approximately 43% of the simulation period) to allow a model spin up period. The model-data comparison result at the sand dunes site was modest ($R^2=0.36$), the predicted water content values were similar except for the higher observed values of soil water content around October 6, 2015 (Figure 12). The mean observed volumetric soil water content for the validation period was 0.6639% and the average water content obtained from the model was 0.6641%. The cumulative actual surface flux (i.e., aggregated value of what actually happens in the surface; evaporation or the infiltration) obtained from the model was only 0.304 mm (Figure 14). The cumulative infiltration was computed to be 0.184 mm at the end of the simulation period, while the cumulative evaporation was 0.714 mm, which is almost four times the cumulative infiltration.

Similarly, the model was run from July 1, 2015 to November 6, 2015 at the gravel plains site. The model output was compared with observations after approximately 50% of the simulation period as model spin-up period. The R^2 value for the simulation was only 0.13 even though the simulated water content values were comparable (Figure 13). The

average observed water content for the calibrated period was 1.482% and the average water content obtained from the model was 1.500%. The modeled water content at the gravel plains had declining slope and did not match the increased water content after October 21, 2015 similar to the sand dunes, hence a lower R^2 value. The simulation at the gravel plains was run for 129 days, and the cumulative actual surface water vapor flux obtained from the model was 8.968 mm (Figure 14). Unlike at the sand dunes, the gravel plains had total evaporation of 8.994 mm which is approximately 1430 times the infiltration (0.0063 mm).

At the gravel plain site with groundwater influence, the cumulative actual surface flux obtained from the model was 24.127 mm (Figure 14) assuming the average water content for the validation period to be 2.97% (approximately twice the water content at the gravel plains site without groundwater influence). With this consideration, the model predicted no infiltration during the period and the entire amount of actual surface flux obtained was from evaporation.

CHAPTER 4: DISCUSSION

4.1 Field observations

It is known that the soil water content increases with rainfall and fog events (Li et al., 2016; Li et al., 2018). The occurrence of fog events during the decline of the soil water content (Figure 2 and 3) when there were no rainfall events suggested the possibility of either advection or radiation fog (locally generated fog) formation at the site. However, these fog events are thought to be more radiative rather than advective. Kaseke et al. (2017) revealed that there are comparable radiation fog and advection fog in the fog zone of the Namib Desert, and more than half of the overall fog events during the study period are not sourced from the ocean. For a fog to be locally-generated, there should be a water source and since the study sites do not have permanent water source except the ephemeral Kuiseb river, the only possible source should be soil moisture and groundwater at the sites.

The relationship between temperature and soil moisture was evaluated to examine the possibility of water vapor movement in this arid environment. In general, there is a positive relationship between soil temperature and soil moisture at both sites (Figure 4, 6, 8, and 10). The relationship between air temperature and soil moisture was similar to the relationship between soil temperature and soil moisture, eliminating the possibility of biased results due to same sensor measuring soil moisture and soil temperature. The temperatures were found to be directly proportional to each other (Figure 2 and 3). There were outliers seen in the analysis of the soil temperature and soil moisture during the overall study period (Figure 4, 6, 8, and 10), which may be attributed to the rainfall events causing substantial change in soil water content over a short period of time. The small number of outliers seen during the analysis of 80 non-rainfall days may further justify the

argument. The soil water content increased with increase in soil temperature at both sites (Figure 4, 6, 8, and 10). A slight exception was seen in this relationship at the gravel plains, where at the lower soil temperature groups, the water content seemed to be a little higher than the following higher temperature groups. Similarly, even though the overall relationship of water content with the soil temperature appeared increasing at the sand dunes, the water content at the lower soil temperature groups was slightly higher than the following soil temperature group, as it was at the gravel plains. The positive relationship between soil water and soil temperature may be due to the process of condensation during the transport of water vapor originated from evaporated soil moisture or groundwater below. During this process, the transported water vapor condenses and adds up moisture to the soil. Condensation also increases soil temperature through the release of latent heat. Because the soil temperature and air temperature followed a similar pattern, it can be deduced that the soil water content would change with soil temperature in a similar way as it does with air temperature.

It is worth noting that the relationship between soil moisture and soil temperature observed in this study contrasts with the one presented by Entekhabi et al. (2001), where it is stated that the water content decreases when there is increase in the near surface soil temperature. The study was done in the Skukuza core site located in Kruger National Park, South Africa, which had an average annual rainfall of 546 mm. However, the setting considered in our study is entirely different than in Entekhabi et al. (2001). The site considered in our study, Gobabeb is extremely dry with average annual precipitation of 7.6 mm. While the annual average rainfall was only around 4.38 mm until 2017, the average raised up to 7.6 mm because of heavy rainfall event in April (11 mm) and May (9.4 mm)

of 2018 (even though the data was available only until June 24, 2018). Generally, there would be a negative relationship between soil temperature and soil moisture in most of the places as seen in the study by Entekhabi et al. (2001). However, based on this study, it suggests that the drier the environment the stronger positive relationship between the soil temperature and soil moisture. Water from soil moisture and shallow groundwater may evaporate easily in a hot and dry environment, hence the strong positive relationship between soil temperature and soil moisture in such an environment, like the Namib Desert. This brings up the fact that the relationship between soil temperature and water content can be different based on the meteorological conditions, and the relationship would be more positive in hot and dry environment as compared to hot and humid environment.

The increase in soil water content with increase in temperature can be explained by a two-step process whereby increased soil temperature leads to loss of surface soil moisture and that in turn causes the movement of water in the form of vapor from the subsoil to the surface soil layers due to the available temperature gradient. The 80 non-rainfall days were mainly considered in order to evaluate if this relationship was valid under both rainfall and without rainfall scenarios, with the assumption that without rainfall there will not be enough water source to increase the soil water content. The only source could have been either fog or the soil moisture and groundwater present in the subsoil. However, since fog events generally occur at lower temperature and during early morning hours, this reasoning favorably points towards the available soil moisture and groundwater. Henceforth, this relationship suggests that the increase in the soil water content may be due to the water vapor transport from the soil moisture or the groundwater available at few meters below the soil surface.

4.2 Modeled water vapor surface fluxes

The use of HYDRUS-1D model for the simulation of actual surface flux is to examine if the process of water vapor transport in the subsoil will lead to some contribution in the formation of non-rainfall waters (Figure 14). The low value of R^2 may be due to the approximation of the soil hydraulic parameters and the heat transport parameters required during the simulation process. Due to the lack of actual field-measured soil hydraulic parameters such as saturated water content and saturated hydraulic conductivity, the Rosetta Lite v.1.1 that is available in HYDRUS-1D model was used to predict the values of these parameters. The residual water content was also predicted by the Rosetta, and was higher than the initial water content observed in the field. However, since HYDRUS-1D model requires the residual water content to be lower than the initial water content to initiate the model run, the residual water content had to be manually attuned and hence a value lower than the initial water content was assigned. The constraints of field measured soil hydraulic parameters may be one of the reasons for the simulated soil water content not being quite synchronized with the observed values.

The thermal conductivity equation and heat transport parameters used in this study are the ones provided by Chung and Horton (1987). The HYDRUS-1D model has the option to choose the thermal conductivity values from either sand, clay or loam options. Because the sites considered in this study are mostly sandy, the heat transport parameters for sand as provided by the model are applied. Further, since temperature at lower boundary was not available in the daily temporal resolution, a constant temperature of 25°C was assumed at the gravel plains because this was the temperature measured at the site near the groundwater depth, and a constant temperature of 24°C was assumed at the sand dunes

since the soil temperature at the sand dunes was found lower than at the gravel plains. This assumption of constant temperature at the lower boundaries may also be a reason for the differences between the modeled and observed water content values.

The validation period was selected after excluding approximately 40% of the overall simulation period in the beginning to make sure that the model reached a stable state. Although in a different way than precipitation, fog also increases the soil water content (Li et al., 2018), but the HYDRUS-1D model does not have a direct option to address any non-rainfall events such as fog or dew. Since the non-rainfall water was not assigned into the model, the possibility of soil moisture recharge by the non-rainfall water was not considered by the model. This may have caused simulated water content values to be lower than the field observed ones (Figure 12 and 13). In addition, water uptake by plants roots was neglected in this study since vegetation cover near the study sites was extremely low. Despite the low abundance of vegetation, if water uptake by plant roots were considered, the soil moisture and actual surface flux probably might have been higher since the presence of a vegetation cover is supposed to increase the soil water content as compared to the bare ground conditions that currently prevail at the study sites (Li et al., 2016).

The actual surface flux at all sites exhibits similar patterns but different magnitudes (Figure 14), and this may be due to the similar meteorological conditions shared by the sites. It is also evident that the surface water vapor flux is lowest at the sand dunes site and is highest at the gravel plains with groundwater access. The actual surface flux at the gravel plains with groundwater presence was modeled by assuming that the average water content at 4 cm below soil surface will be twice as it was at the gravel plains site without

groundwater at similar depth. Similarly, at the gravel plains without groundwater access, the actual surface flux of water vapor obtained from the model was higher than at the sand dunes site (Figure 14), which may be due to the difference in soil texture. The sand dunes site has 74.8% of sand while both the gravel plains sites have more than 90% of sand. The infiltration rate is based on soil texture, and the coarser the texture the higher the infiltration rate (Mazaheri and Mahmoodabadi, 2012). This illustrates that the higher the sand content compared to silt and clay, the easier it is for water to move through the pore spaces. Hence, there is greater movement of water vapor in the subsoil at the gravel plains sites where the sand content is higher, than at the sand dunes site where the sand content is comparatively lower.

The actual surface flux and evaporation values as obtained from the HYDRUS-1D model clearly depicts that there is some amount of water vapor exchange throughout the period from the soil to the atmosphere, and this will have contributed to the formation of radiation fog as well as mixed fog in the area. The positive flux of water vapor at the soil surface suggest a constant transfer of soil water near the surface to the atmosphere, and over time this cumulated water vapor under favorable meteorological conditions may lead to the formation of fog. The model results further underscores that, at sites where groundwater is present, the transfer of water vapor to the atmosphere can be much greater and hence fog formation can become more significant in these settings compared to sites where groundwater is absent or too deep.

CHAPTER 5: CONCLUSIONS

Soil moisture and groundwater can be a potential source of non-rainfall waters such as fog and dew in dryland ecosystems like the Namib Desert. The field observation analysis showed that there was an increase in volumetric soil water content near soil surface with increase in soil temperature, which is a new finding, and an important piece of evidence of the biophysical basis of water vapor movement. The relationship was similar during the entire study period as well as for a rainless period of 80 days. The study results documented the transfer of water vapor in amount sufficient to support the formation of non-rainfall waters at the study sites selected for this research. Field observations supported by the results of hydrological modeling have demonstrated the possible contribution of groundwater and soil moisture to non-rainfall waters formation through water vapor movement. This research has for the first time demonstrated the possibility for subsoil waters (soil moisture and groundwater) to participate in the formation of non-rainfall waters, specifically radiation fog in the Namib Desert. The modeling results suggest that this approach can be further utilized to study possible non-rainfall water sources in other areas where sources of water are very inadequate.

TABLES

Table 1. Soil hydraulic parameters used in the HYDRUS-1D model for three sites: sand dunes, gravel plains, and gravel plains with groundwater presence (Gravel plains (GW)).

Soil Hydraulic Parameters	Sand dunes	Gravel plains	Gravel plains (GW)
Residual water content, Q_r [-]	0.001	0.01	0.01
Saturated water content, Q_s [-]	0.3886	0.3865	0.3819
Parameter alpha [1/cm]	0.034	0.038	0.02
Parameter n [-]	1.558	3.35	1.915
Saturated hydraulic conductivity, K_s [cm/days]	70.01	428.95	445.25
Parameter, l [-]	0.5	0.5	0.5

Table 2. Heat transport parameters used in the HYDRUS-1D model for three sites: sand dunes, gravel plains, and gravel plains with groundwater presence (Gravel plains (GW)).

Heat transport parameters	Sand dunes	Gravel plains	Gravel plains (GW)
Volume fraction of solid phase	0.6114	0.6135	0.6181
Volume fraction of organic matter	0	0	0
Longitudinal thermal dispersivity	5	5	5
Coefficient b1 for thermal conductivity function	1.47E+16	1.47E+16	1.47E+16
Coefficient b2 for thermal conductivity function	-1.55E+17	-1.55E+17	-1.55E+17
Coefficient b3 for thermal conductivity function	3.17E+17	3.17E+17	3.17E+17
Volumetric heat capacity of solid phase (Cn)	1.43E+14	1.43E+14	1.43E+14
Volumetric heat capacity of organic matter (Co)	1.87E+14	1.87E+14	1.87E+14
Volumetric heat capacity of liquid phase (Cw)	3.12E+14	3.12E+14	3.12E+14

Table 3. Descriptive statistics of volumetric water content from field observations for the overall study period and the 80 non-rainfall days at sand dunes and gravel plains.

Statistics	Overall study period		80 non-rainfall days (Aug.19 – Nov. 6, 2015)	
	Sand dunes	Gravel plains	Sand dunes	Gravel plains
Mean (%)	0.771	2.105	0.639	1.499
Std. Dev. (%)	0.52	1.24	0.05	0.07
Kurtosis (k-value)	34.82	18.52	0.47	1.2
Skewness	4.95	3.9	-0.54	0.73

Table 4. Statistics of volumetric water content, rainfall and fog for different hydrologic years at sand dunes and gravel plains.

Year	VWC_GP		VWC_SD		Rain (mm)				Fog (mm)			
	Mean	Std. Dev.	Mean	Std. Dev.	rainfall days	Sum	Mean	Std. Dev.	fog days	Sum	Mean	Std. Dev.
2013-2014*	0.018	0.002	NA	NA	2	0.5	0.002	0.022	NA	NA	NA	NA
2014-2015	0.020	0.011	0.006	0.001	4	4.3	0.012	0.143	63	142.62	0.493	0.011
2015-2016	0.019	0.010	0.007	0.002	2	6.6	0.018	0.325	76	174.30	0.480	0.010
2016-2017	0.020	0.011	0.006	0.003	4	3.6	0.010	0.124	45	81.46	0.288	0.011
2017-2018**	0.029	0.020	0.011	0.009	6	23.0	0.086	0.709	NA	NA	NA	NA
<p><u>Note:</u> VWC_GP = Volumetric water content at the gravel plains, VWC_SD = Volumetric water content at the sand dunes, Std. Dev. = Standard deviation, NA = Not available *started from 12/29/2013, **ended on 6/24/2018 One hydrologic year = October 1 to September 30</p>												

FIGURES

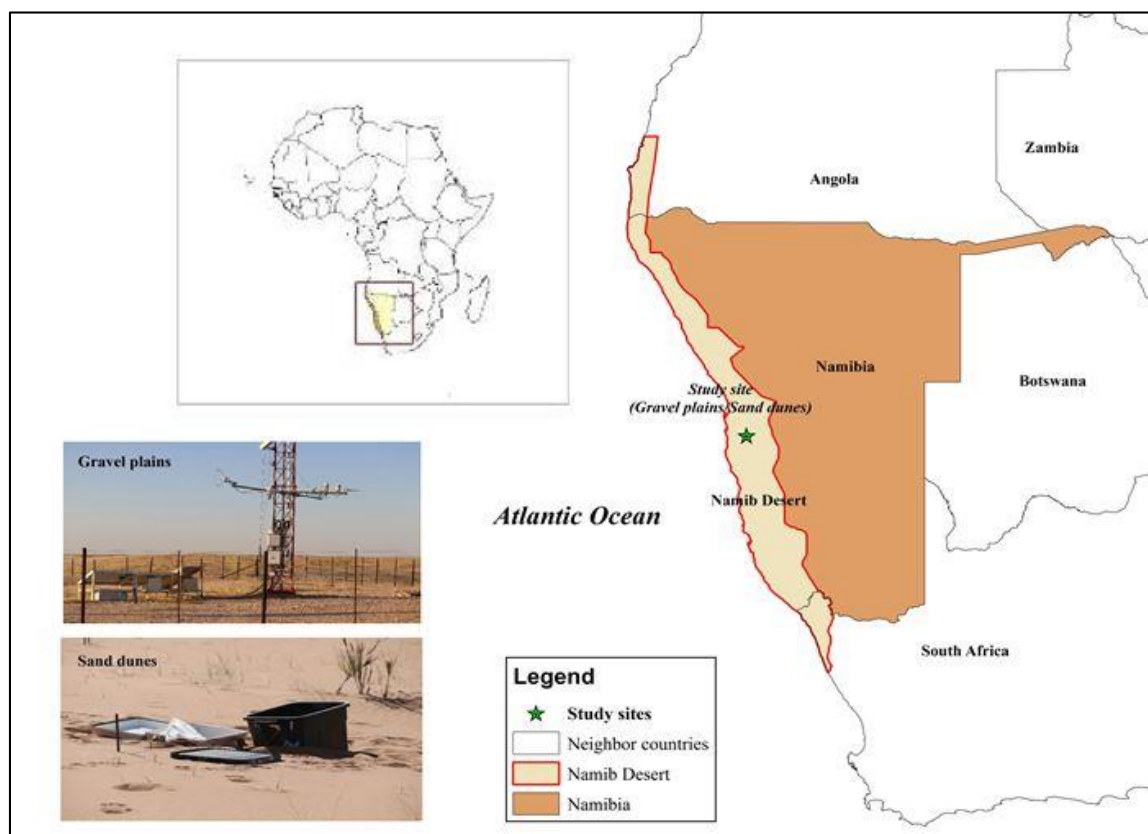


Figure 1. Extent of the Namib Desert and study site locations. The map shows the location of study sites, extent of Namib Desert, and two images taken at the site showing general characteristics of the study area.

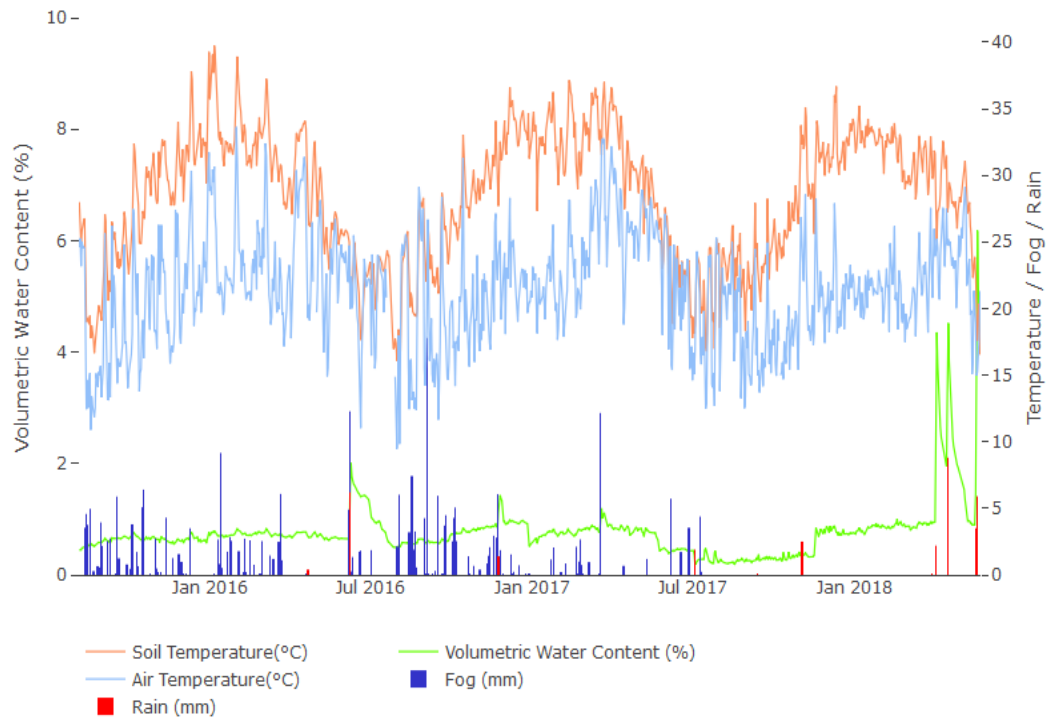


Figure 2. Variation of different variables (soil temperature, air temperature, volumetric water content, fog and rain) at sand dunes from August 5, 2015 to May 22, 2018.

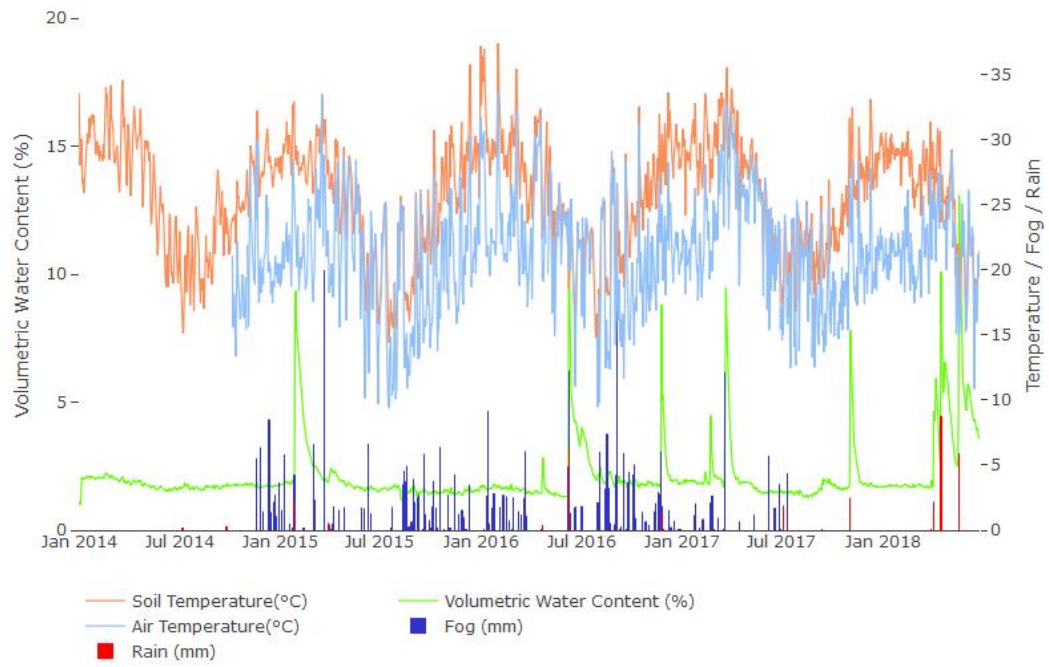


Figure 3. Variation of different variables (soil temperature, air temperature, volumetric water content, fog and rain) at gravel plains from December 29, 2013 to June 24, 2018.

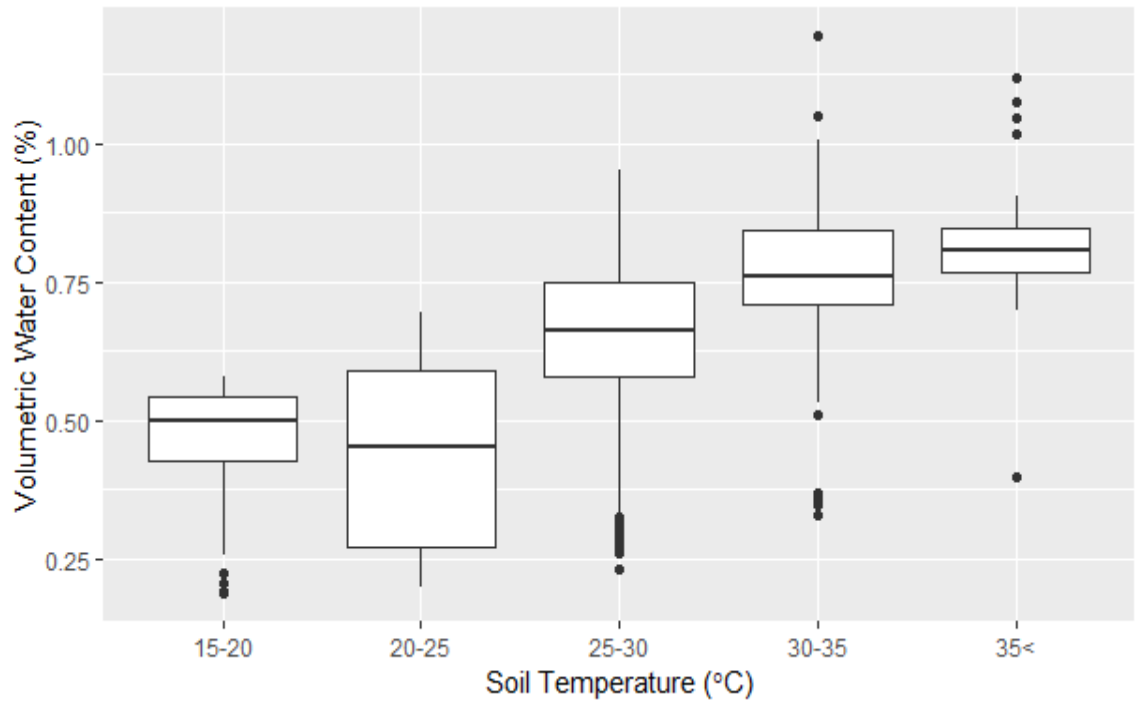


Figure 4. Relationship of volumetric water content with soil temperature at sand dunes from August 5, 2015 to May 22, 2018.

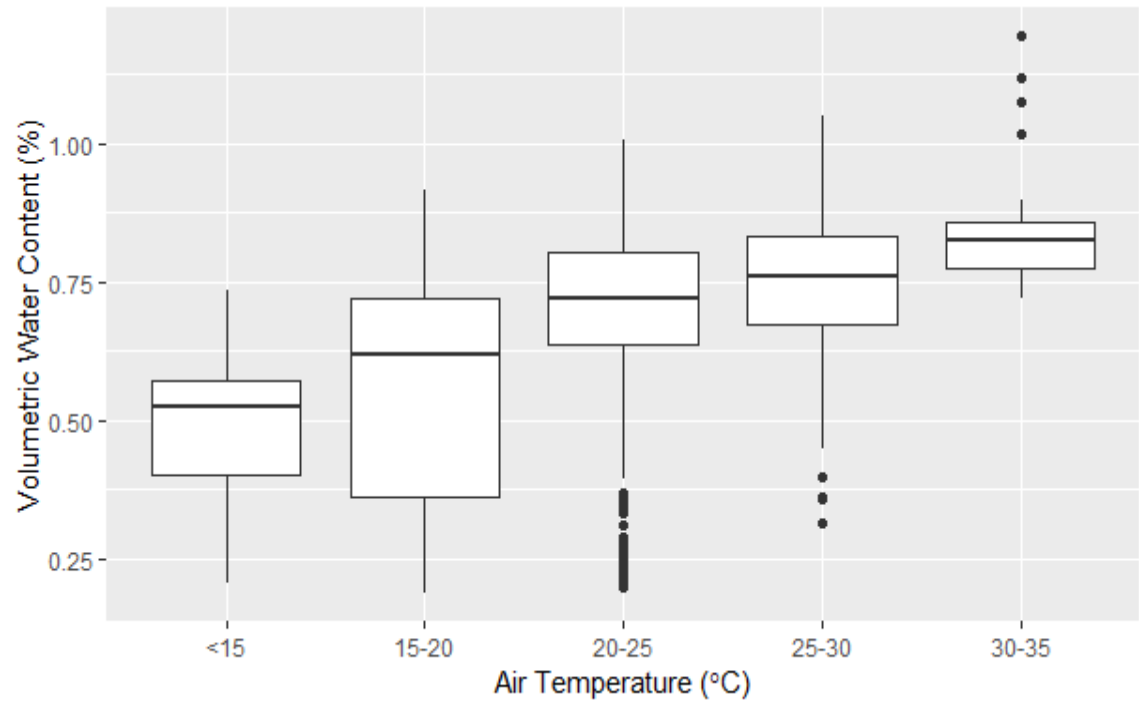


Figure 5. Relationship of volumetric water content with air temperature at sand dunes from August 5, 2015 to May 22, 2018.

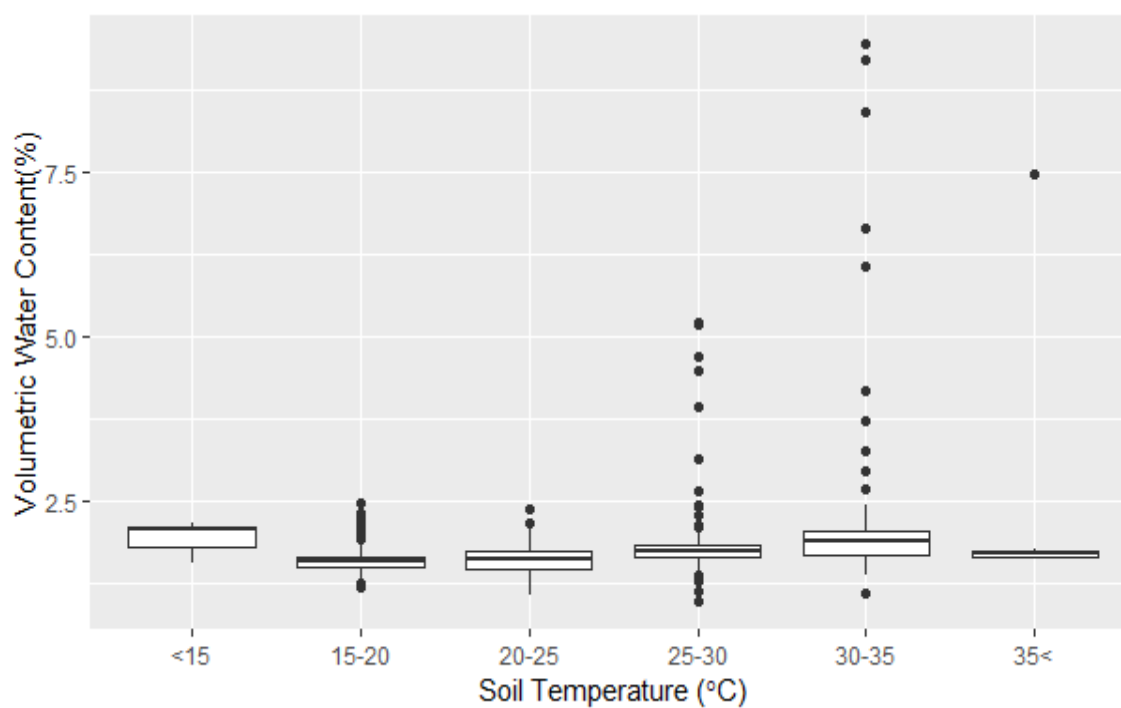


Figure 6. Relationship of volumetric water content with soil temperature at gravel plains from December 29, 2013 to June 24, 2018.

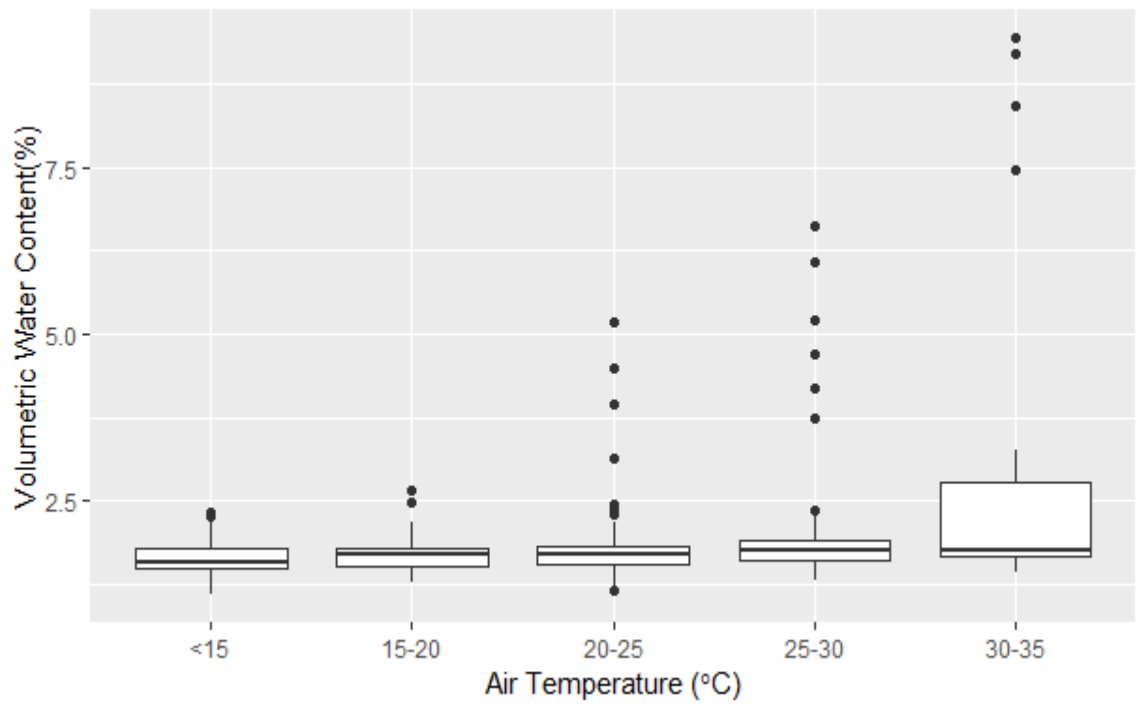


Figure 7. Relationship of volumetric water content with air temperature at gravel plains from December 29, 2013 to June 24, 2018.

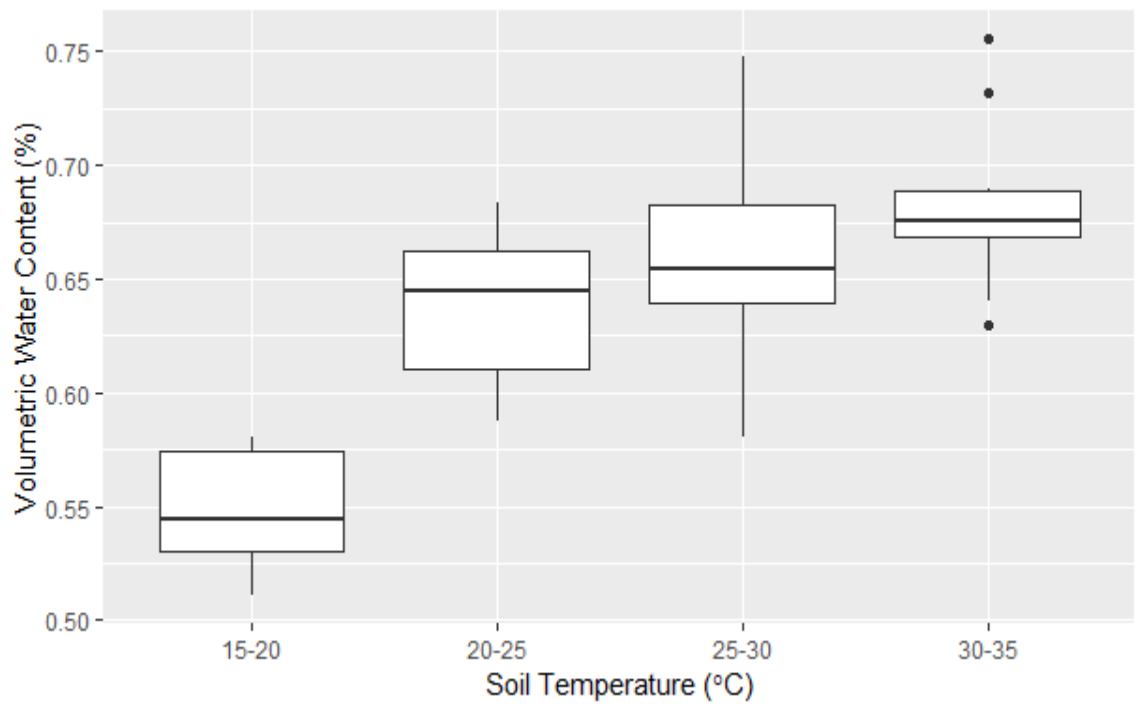


Figure 8. Relationship of volumetric water content with soil temperature at sand dunes for 80 non-rainfall days from August 19, 2015 to November 06, 2015.

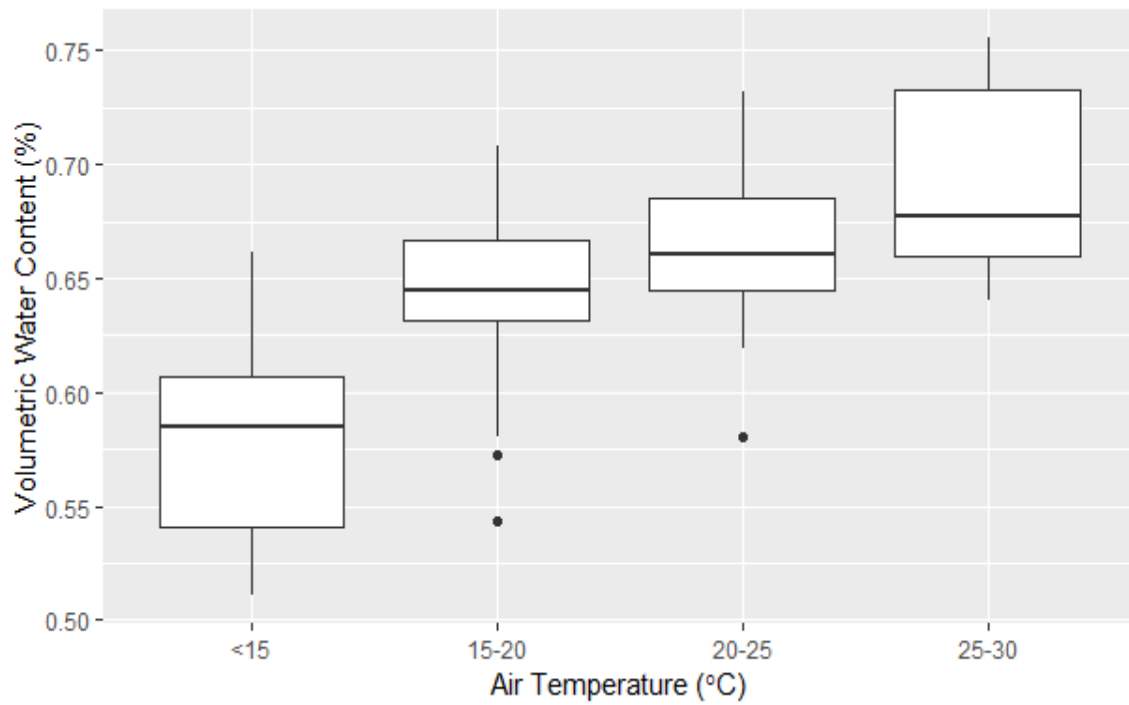


Figure 9. Relationship of volumetric water content with air temperature at sand dunes for 80 non-rainfall days from August 19, 2015 to November 06, 2015.

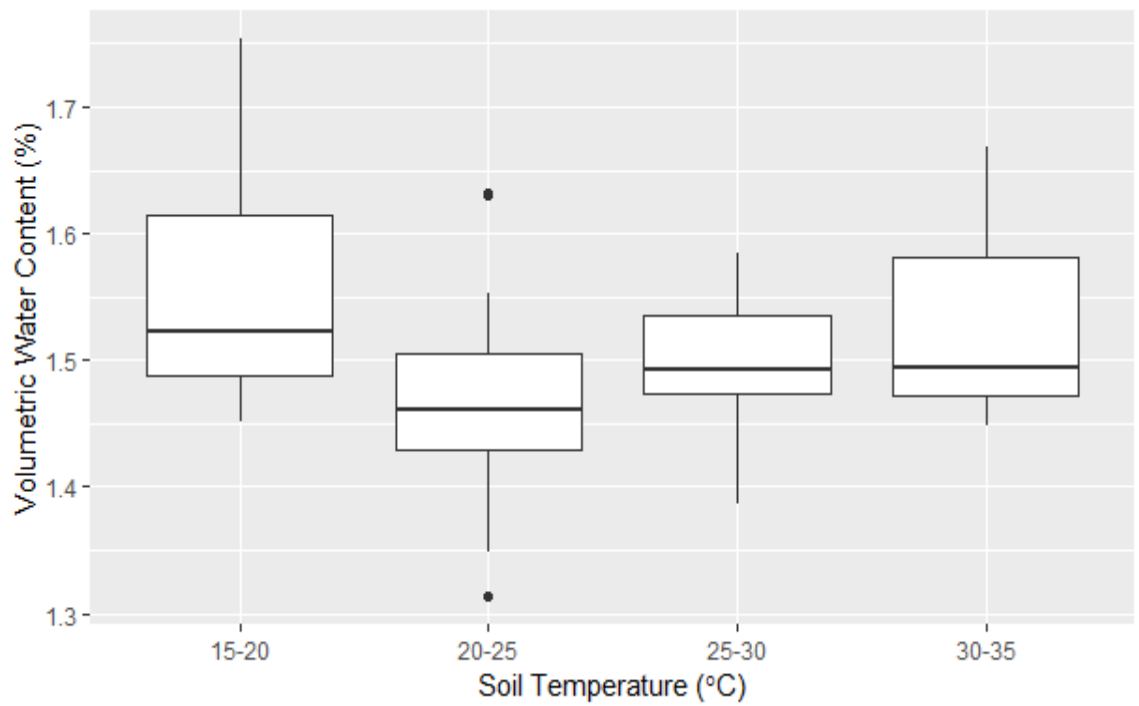


Figure 10. Relationship of volumetric water content with soil temperature at gravel plains from August 19, 2015 to November 06, 2015.

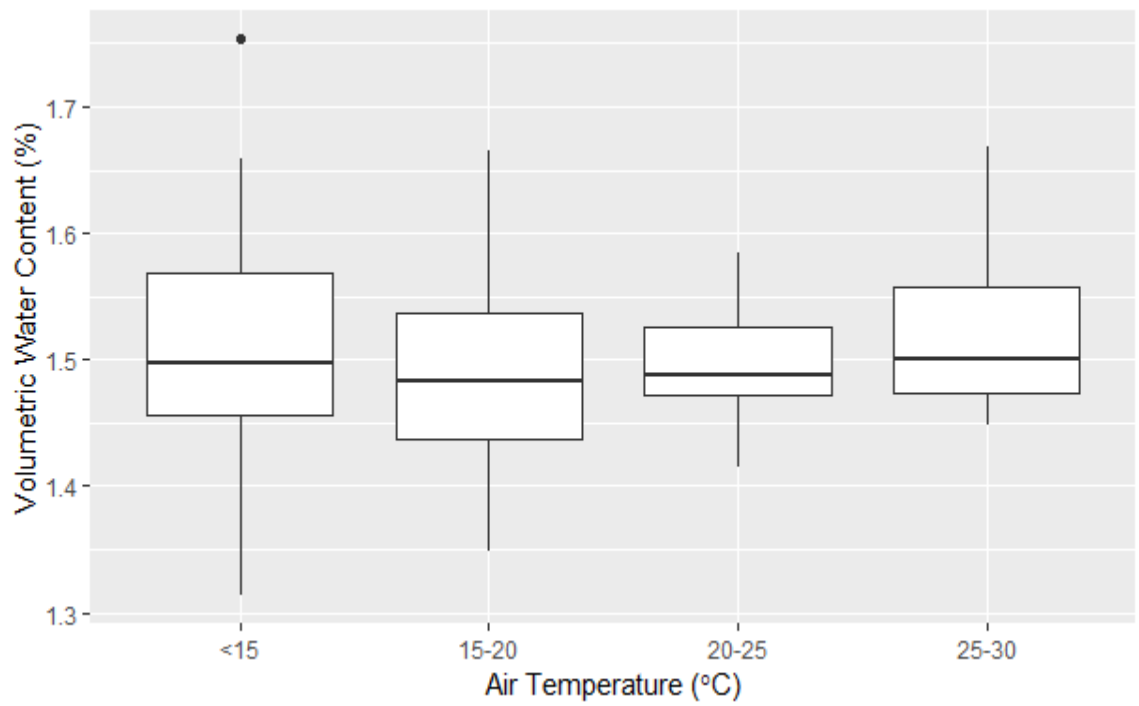


Figure 11. Relationship of volumetric water content with air temperature at gravel plains from August 19, 2015 to November 06, 2015.

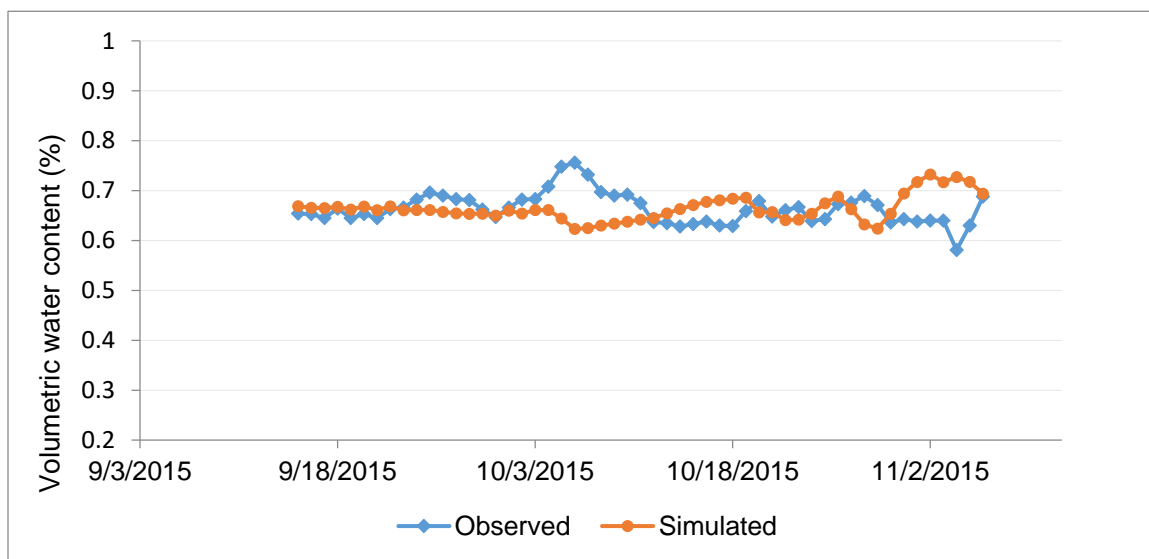


Figure 12. Observed and simulated volumetric water content at sand dunes.

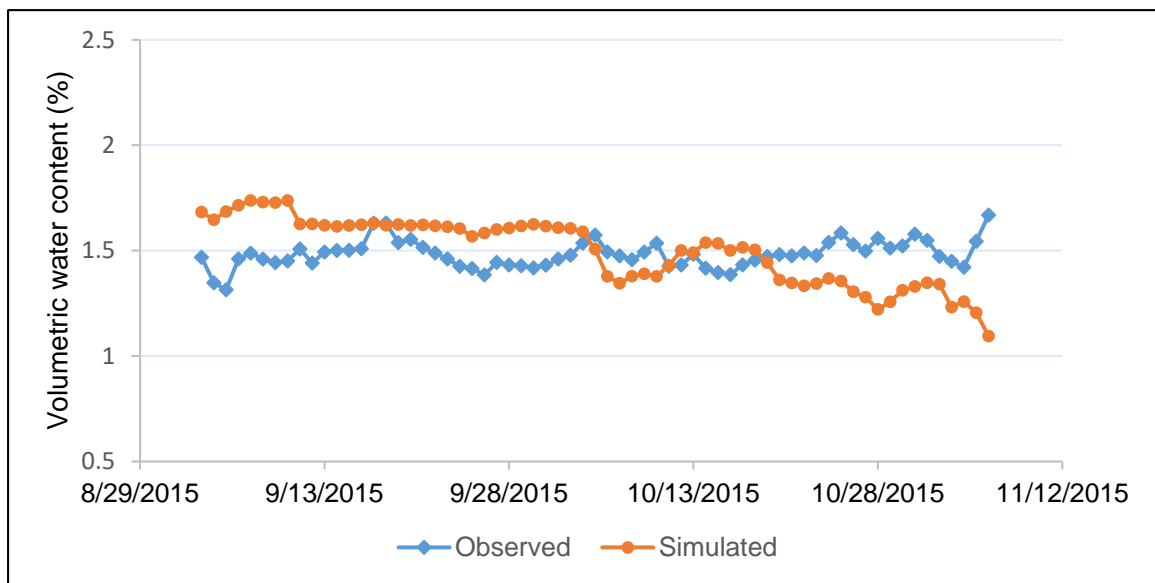


Figure 13. Observed and simulated volumetric water content at gravel plains.

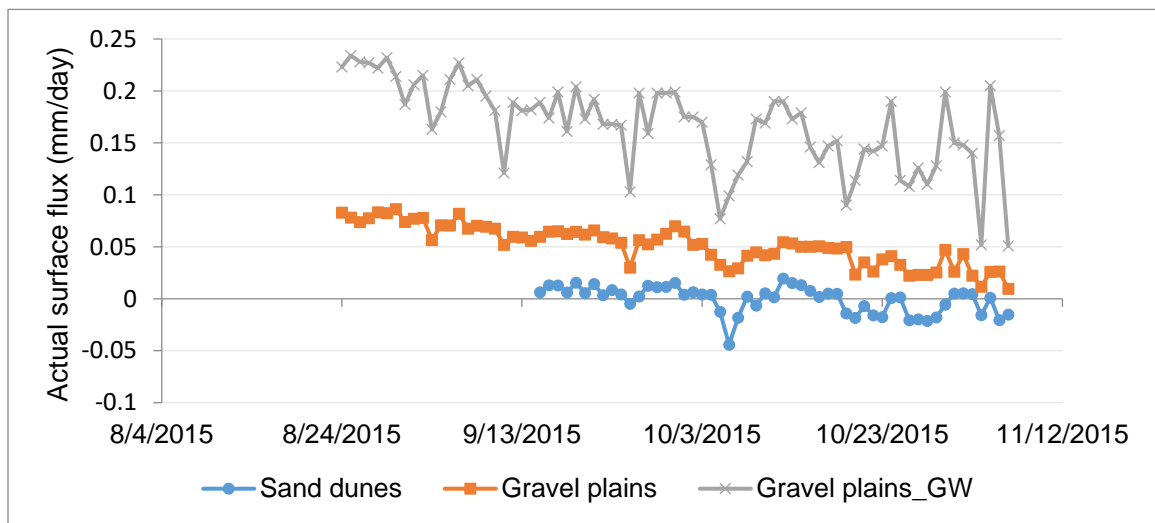


Figure 14. Actual surface flux (mm/day) obtained from HYDRUS-1D model at sand dunes, gravel plains, and gravel plains with groundwater presence (Gravel plains_GW).

APPENDICES

Appendix A: Volumetric water content, rainfall and fog patterns at gravel plains and sand dunes

Date	Gravel plains VWC (%)	Sand dunes VWC (%)	Rain (mm)	Fog (mm)
7/1/2015	1.555	NA	0.00	NA
7/2/2015	1.564	NA	0.00	NA
7/3/2015	1.610	NA	0.00	NA
7/4/2015	1.628	NA	0.00	NA
7/5/2015	1.636	NA	0.00	NA
7/6/2015	1.639	NA	0.00	NA
7/7/2015	1.668	NA	0.00	NA
7/8/2015	1.665	NA	0.00	NA
7/9/2015	1.661	NA	0.00	NA
7/10/2015	1.664	NA	0.00	NA
7/11/2015	1.592	NA	0.00	NA
7/12/2015	1.556	NA	0.00	NA
7/13/2015	1.549	NA	0.00	NA
7/14/2015	1.555	NA	0.00	NA
7/15/2015	1.566	NA	0.00	NA
7/16/2015	1.577	NA	0.00	NA
7/17/2015	1.623	NA	0.00	NA
7/18/2015	1.646	NA	0.00	0.00
7/19/2015	1.655	NA	0.00	0.00
7/20/2015	1.605	NA	0.00	0.16
7/21/2015	1.622	NA	0.00	1.78

7/22/2015	1.647	NA	0.00	0.44
7/23/2015	1.701	NA	0.00	0.00
7/24/2015	1.731	NA	0.00	0.00
7/25/2015	1.717	NA	0.00	0.00
7/26/2015	1.786	NA	0.00	0.00
7/27/2015	1.729	NA	0.00	0.00
7/28/2015	1.653	NA	0.00	0.00
7/29/2015	1.653	NA	0.00	0.00
7/30/2015	1.631	NA	0.00	0.00
7/31/2015	1.669	NA	0.00	0.00
8/1/2015	1.765	NA	0.00	0.00
8/2/2015	1.724	NA	0.00	0.00
8/3/2015	1.671	NA	0.00	0.00
8/4/2015	1.645	NA	0.00	0.00
8/5/2015	1.596	0.448	0.00	0.00
8/6/2015	1.313	0.457	0.00	0.00
8/7/2015	1.194	0.447	0.00	0.00
8/8/2015	1.200	0.483	0.00	0.00
8/9/2015	1.188	0.494	0.00	0.00
8/10/2015	1.149	0.492	0.00	0.00
8/11/2015	1.142	0.501	0.00	3.54
8/12/2015	1.085	0.489	0.00	0.70
8/13/2015	1.217	0.523	0.00	4.58
8/14/2015	1.270	0.506	0.00	0.00
8/15/2015	1.316	0.549	0.00	3.76
8/16/2015	1.331	0.524	0.00	0.00
8/17/2015	1.361	0.517	0.00	0.00

8/18/2015	1.413	0.549	0.00	4.96
8/19/2015	1.508	0.558	0.00	0.00
8/20/2015	1.461	0.531	0.00	0.00
8/21/2015	1.468	0.513	0.00	0.28
8/22/2015	1.522	0.511	0.00	0.28
8/23/2015	1.549	0.529	0.00	0.00
8/24/2015	1.498	0.543	0.00	0.00
8/25/2015	1.509	0.544	0.00	0.00
8/26/2015	1.658	0.578	0.00	0.66
8/27/2015	1.666	0.588	0.00	0.64
8/28/2015	1.598	0.580	0.00	0.56
8/29/2015	1.565	0.573	0.00	0.00
8/30/2015	1.656	0.577	0.00	3.94
8/31/2015	1.754	0.597	0.00	2.18
9/1/2015	1.615	0.599	0.00	0.00
9/2/2015	1.524	0.619	0.00	0.00
9/3/2015	1.468	0.658	0.00	0.00
9/4/2015	1.348	0.640	0.00	0.00
9/5/2015	1.314	0.605	0.00	0.00
9/6/2015	1.461	0.593	0.00	2.54
9/7/2015	1.488	0.591	0.00	0.00
9/8/2015	1.460	0.612	0.00	0.00
9/9/2015	1.443	0.612	0.00	2.74
9/10/2015	1.451	0.598	0.00	0.00
9/11/2015	1.508	0.666	0.00	0.00
9/12/2015	1.441	0.644	0.00	0.00
9/13/2015	1.493	0.651	0.00	0.00

9/14/2015	1.501	0.659	0.00	0.00
9/15/2015	1.502	0.654	0.00	0.10
9/16/2015	1.509	0.653	0.00	0.02
9/17/2015	1.630	0.645	0.00	5.88
9/18/2015	1.631	0.664	0.00	0.00
9/19/2015	1.538	0.645	0.00	1.24
9/20/2015	1.553	0.653	0.00	0.22
9/21/2015	1.515	0.645	0.00	0.00
9/22/2015	1.489	0.663	0.00	0.00
9/23/2015	1.461	0.666	0.00	0.00
9/24/2015	1.426	0.682	0.00	0.00
9/25/2015	1.415	0.696	0.00	0.00
9/26/2015	1.385	0.690	0.00	0.00
9/27/2015	1.444	0.683	0.00	0.00
9/28/2015	1.432	0.681	0.00	0.78
9/29/2015	1.428	0.662	0.00	0.16
9/30/2015	1.418	0.647	0.00	0.00
10/1/2015	1.431	0.666	0.00	0.00
10/2/2015	1.460	0.682	0.00	0.46
10/3/2015	1.478	0.683	0.00	1.82
10/4/2015	1.536	0.708	0.00	3.80
10/5/2015	1.574	0.748	0.00	0.00
10/6/2015	1.494	0.756	0.00	0.00
10/7/2015	1.475	0.732	0.00	0.00
10/8/2015	1.457	0.697	0.00	0.00
10/9/2015	1.493	0.690	0.00	1.72
10/10/2015	1.535	0.692	0.00	0.66

10/11/2015	1.426	0.675	0.00	0.16
10/12/2015	1.432	0.637	0.00	0.00
10/13/2015	1.483	0.635	0.00	0.00
10/14/2015	1.417	0.628	0.00	0.00
10/15/2015	1.396	0.633	0.00	0.00
10/16/2015	1.386	0.638	0.00	5.08
10/17/2015	1.433	0.630	0.00	6.40
10/18/2015	1.455	0.629	0.00	0.00
10/19/2015	1.472	0.659	0.00	0.00
10/20/2015	1.481	0.679	0.00	0.00
10/21/2015	1.475	0.648	0.00	0.00
10/22/2015	1.489	0.661	0.00	0.00
10/23/2015	1.477	0.667	0.00	0.00
10/24/2015	1.539	0.639	0.00	0.02
10/25/2015	1.584	0.643	0.00	0.00
10/26/2015	1.528	0.673	0.00	0.00
10/27/2015	1.498	0.676	0.00	0.00
10/28/2015	1.558	0.689	0.00	0.00
10/29/2015	1.513	0.671	0.00	0.00
10/30/2015	1.522	0.636	0.00	0.00
10/31/2015	1.578	0.643	0.00	2.74
11/1/2015	1.549	0.638	0.00	0.48
11/2/2015	1.473	0.640	0.00	0.00
11/3/2015	1.449	0.640	0.00	0.16
11/4/2015	1.421	0.581	0.00	0.00
11/5/2015	1.544	0.630	0.00	0.20
11/6/2015	1.669	0.688	0.00	0.00

Appendix B: Volumetric water content, soil temperature and air temperature patterns at gravel plains and sand dunes.

Date	Gravel plains		Sand dunes		Air Temp (°C)
	VWC (%)	Soil Temp (°C)	VWC (%)	Soil Temp (°C)	
7/1/2015	1.555	18.35	NA	NA	NA
7/2/2015	1.564	19.13	NA	NA	NA
7/3/2015	1.610	21.39	NA	NA	NA
7/4/2015	1.628	22.50	NA	NA	NA
7/5/2015	1.636	22.79	NA	NA	NA
7/6/2015	1.639	23.02	NA	NA	NA
7/7/2015	1.668	24.34	NA	NA	NA
7/8/2015	1.665	24.33	NA	NA	NA
7/9/2015	1.661	24.37	NA	NA	NA
7/10/2015	1.664	24.95	NA	NA	NA
7/11/2015	1.592	21.94	NA	NA	NA
7/12/2015	1.556	19.22	NA	NA	NA
7/13/2015	1.549	17.66	NA	NA	NA
7/14/2015	1.555	16.69	NA	NA	NA
7/15/2015	1.566	15.34	NA	NA	NA
7/16/2015	1.577	14.40	NA	NA	NA
7/17/2015	1.623	15.80	NA	NA	NA
7/18/2015	1.646	16.84	NA	NA	0.00
7/19/2015	1.655	17.74	NA	NA	0.00
7/20/2015	1.605	16.56	NA	NA	0.16
7/21/2015	1.622	16.31	NA	NA	1.78

7/22/2015	1.647	15.64	NA	NA	0.44
7/23/2015	1.701	16.72	NA	NA	0.00
7/24/2015	1.731	16.65	NA	NA	0.00
7/25/2015	1.717	15.50	NA	NA	0.00
7/26/2015	1.786	19.04	NA	NA	0.00
7/27/2015	1.729	18.31	NA	NA	0.00
7/28/2015	1.653	16.46	NA	NA	0.00
7/29/2015	1.653	16.73	NA	NA	0.00
7/30/2015	1.631	15.59	NA	NA	0.00
7/31/2015	1.669	17.05	NA	NA	0.00
8/1/2015	1.765	21.64	NA	NA	0.00
8/2/2015	1.724	21.62	NA	NA	0.00
8/3/2015	1.671	20.73	NA	NA	0.00
8/4/2015	1.645	20.15	NA	NA	0.00
8/5/2015	1.596	22.29	0.448	27.99	0.00
8/6/2015	1.313	25.68	0.457	26.25	0.00
8/7/2015	1.194	23.01	0.447	24.72	0.00
8/8/2015	1.200	24.71	0.483	25.87	0.00
8/9/2015	1.188	24.97	0.494	26.39	0.00
8/10/2015	1.149	24.31	0.492	26.60	0.00
8/11/2015	1.142	24.90	0.501	26.77	3.54
8/12/2015	1.085	20.62	0.489	22.46	0.70
8/13/2015	1.217	18.04	0.523	19.03	4.58
8/14/2015	1.270	18.16	0.506	19.30	0.00
8/15/2015	1.316	18.28	0.549	19.08	3.76
8/16/2015	1.331	17.64	0.524	18.83	0.00
8/17/2015	1.361	18.26	0.517	19.45	0.00

8/18/2015	1.413	16.91	0.549	17.77	4.96
8/19/2015	1.508	18.10	0.558	18.72	0.00
8/20/2015	1.461	16.90	0.531	18.28	0.00
8/21/2015	1.468	16.80	0.513	17.78	0.28
8/22/2015	1.522	16.07	0.511	16.66	0.28
8/23/2015	1.549	16.65	0.529	17.51	0.00
8/24/2015	1.498	17.29	0.543	18.60	0.00
8/25/2015	1.509	18.05	0.544	19.26	0.00
8/26/2015	1.658	19.11	0.578	19.48	0.66
8/27/2015	1.666	19.50	0.588	20.22	0.64
8/28/2015	1.598	18.71	0.580	19.86	0.56
8/29/2015	1.565	18.96	0.573	19.64	0.00
8/30/2015	1.656	18.12	0.577	19.08	3.94
8/31/2015	1.754	19.85	0.597	20.46	2.18
9/1/2015	1.615	19.39	0.599	20.71	0.00
9/2/2015	1.524	21.84	0.619	23.07	0.00
9/3/2015	1.468	25.95	0.658	27.08	0.00
9/4/2015	1.348	24.43	0.640	26.53	0.00
9/5/2015	1.314	20.66	0.605	23.54	0.00
9/6/2015	1.461	19.81	0.593	21.56	2.54
9/7/2015	1.488	19.35	0.591	20.58	0.00
9/8/2015	1.460	20.51	0.612	22.11	0.00
9/9/2015	1.443	20.32	0.612	21.91	2.74
9/10/2015	1.451	19.67	0.598	21.23	0.00
9/11/2015	1.508	25.84	0.666	26.51	0.00
9/12/2015	1.441	23.56	0.644	25.30	0.00
9/13/2015	1.493	23.83	0.651	25.25	0.00

9/14/2015	1.501	24.28	0.659	25.74	0.00
9/15/2015	1.502	23.46	0.654	24.94	0.10
9/16/2015	1.509	22.48	0.653	24.30	0.02
9/17/2015	1.630	21.55	0.645	23.11	5.88
9/18/2015	1.631	22.54	0.664	24.24	0.00
9/19/2015	1.538	21.33	0.645	22.97	1.24
9/20/2015	1.553	22.17	0.653	23.67	0.22
9/21/2015	1.515	21.54	0.645	23.16	0.00
9/22/2015	1.489	22.04	0.663	24.00	0.00
9/23/2015	1.461	22.53	0.666	24.60	0.00
9/24/2015	1.426	23.66	0.682	25.64	0.00
9/25/2015	1.415	26.21	0.696	27.25	0.00
9/26/2015	1.385	24.62	0.690	26.72	0.00
9/27/2015	1.444	23.39	0.683	25.46	0.00
9/28/2015	1.432	22.47	0.681	24.77	0.78
9/29/2015	1.428	21.02	0.662	23.38	0.16
9/30/2015	1.418	20.46	0.647	22.57	0.00
10/1/2015	1.431	21.50	0.666	23.78	0.00
10/2/2015	1.460	22.25	0.682	24.69	0.46
10/3/2015	1.478	22.76	0.683	24.90	1.82
10/4/2015	1.536	24.48	0.708	26.12	3.80
10/5/2015	1.574	28.47	0.748	29.27	0.00
10/6/2015	1.494	30.76	0.756	32.38	0.00
10/7/2015	1.475	29.70	0.732	31.74	0.00
10/8/2015	1.457	26.97	0.697	29.74	0.00
10/9/2015	1.493	26.44	0.690	29.16	1.72
10/10/2015	1.535	26.69	0.692	28.61	0.66

10/11/2015	1.426	24.07	0.675	27.77	0.16
10/12/2015	1.432	21.85	0.637	24.92	0.00
10/13/2015	1.483	23.10	0.635	24.87	0.00
10/14/2015	1.417	22.10	0.628	24.89	0.00
10/15/2015	1.396	23.38	0.633	25.74	0.00
10/16/2015	1.386	25.17	0.638	27.32	5.08
10/17/2015	1.433	24.44	0.630	26.99	6.40
10/18/2015	1.455	24.59	0.629	26.74	0.00
10/19/2015	1.472	27.46	0.659	29.15	0.00
10/20/2015	1.481	28.69	0.679	30.66	0.00
10/21/2015	1.475	27.78	0.648	29.81	0.00
10/22/2015	1.489	28.02	0.661	29.93	0.00
10/23/2015	1.477	27.07	0.667	30.29	0.00
10/24/2015	1.539	25.30	0.639	28.51	0.02
10/25/2015	1.584	26.46	0.643	28.46	0.00
10/26/2015	1.528	28.72	0.673	30.42	0.00
10/27/2015	1.498	28.92	0.676	30.80	0.00
10/28/2015	1.558	29.87	0.689	31.68	0.00
10/29/2015	1.513	27.33	0.671	30.51	0.00
10/30/2015	1.522	25.24	0.636	28.41	0.00
10/31/2015	1.578	25.45	0.643	28.24	2.74
11/1/2015	1.549	24.99	0.638	27.86	0.48
11/2/2015	1.473	25.86	0.640	28.08	0.00
11/3/2015	1.449	30.39	0.640	31.78	0.16
11/4/2015	1.421	27.15	0.581	29.85	0.00
11/5/2015	1.544	28.76	0.630	30.86	0.20
11/6/2015	1.669	31.09	0.688	31.68	0.00

REFERENCES

- Adeel, Z., U. Safriel, D. Niemeijer and R. White (2005). Ecosystems and human well-being: desertification synthesis, World Resources Institute (WRI).
- Bergot, T. and D. Guedalia (1994). "Numerical forecasting of radiation fog. Part I: Numerical model and sensitivity tests." Monthly Weather Review **122**(6): 1218-1230.
- Bittelli, M., F. Ventura, G. S. Campbell, R. L. Snyder, F. Gallegati and P. R. Pisa (2008). "Coupling of heat, water vapor, and liquid water fluxes to compute evaporation in bare soils." Journal of Hydrology **362**(3): 191-205.
- Bristow, C. S., G. Duller and N. Lancaster (2007). "Age and dynamics of linear dunes in the Namib Desert." Geology **35**(6): 555-558.
- Cahill, A. T. and M. B. Parlange (1998). "On water vapor transport in field soils." Water Resources Research **34**(4): 731-739.
- Chung, S. O. and R. Horton (1987). "Soil heat and water flow with a partial surface mulch." Water Resources Research **23**(12): 2175-2186.
- D'Odorico, P. and A. Porporato (2006). Dryland ecohydrology, Springer.
- Dawson, T. E. (1998). "Fog in the California redwood forest: ecosystem inputs and use by plants." Oecologia **117**(4): 476-485.
- Eckardt, F., K. Soderberg, L. Coop, A. Muller, K. Vickery, R. Grandin, C. Jack, T. Kapalanga and J. Henschel (2013). "The nature of moisture at Gobabeb, in the central Namib Desert." Journal of Arid Environments **93**: 7-19.
- Eltahir, E. A. (1998). "A soil moisture–rainfall feedback mechanism: 1. Theory and observations." Water Resources Research **34**(4): 765-776.

- Entekhabi, D., J. L. Privette and J. A. Berry (2001). Assessing the relationship between surface temperature and soil moisture in southern Africa. Remote Sensing and Hydrology 2000: A Selection of Papers Presented at the Conference on Remote Sensing and Hydrology 2000, Held at Santa Fe, New Mexico, USA, April 2000, International Assn of Hydrological Sciences.
- Eugster, W. (2008). "Fog research." Die Erde **139**(1-2): 1-10.
- Ingraham, N. L. and R. A. Matthews (1988). "Fog drip as a source of groundwater recharge in northern Kenya." Water Resources Research **24**(8): 1406-1410.
- Ingraham, N. L. and R. A. Matthews (1995). "The importance of fog-drip water to vegetation: Point Reyes Peninsula, California." Journal of Hydrology **164**(1-4): 269-285.
- Kaseke, K. F. (2009). Non-rainfall Atmospheric Water in Arid Soil Microhydrology and Ecology, MSc thesis, Univ. of Stellenbosch, Stellenbosch, South Africa.
- Kaseke, K. F. (2018). A Stable Isotope Approach to Investigative Ecohydrological Processes in Namibia.
- Kaseke, K. F. and L. Wang (2018). "Fog and dew as potable water resources: Maximizing harvesting potential and water quality concerns." GeoHealth **2**(10): 327-332.
- Kaseke, K. F., L. Wang and M. K. Seely (2017). "Nonrainfall water origins and formation mechanisms." Science Advances **3**(3): e1603131.
- Kaseke, K. F., L. Wang, H. Wanke, C. Tian, M. Lanning and W. Jiao (2018). "Precipitation origins and key drivers of precipitation isotope (^{18}O , ^2H , and ^{17}O) compositions over windhoek." Journal of Geophysical Research: Atmospheres **123**(14): 7311-7330.

- Khire, M. V., C. H. Benson and P. J. Bosscher (1997). "Water balance modeling of earthen final covers." Journal of Geotechnical and Geoenvironmental Engineering **123**(8): 744-754.
- Klemm, O., R. S. Schemenauer, A. Lummerich, P. Cereceda, V. Marzol, D. Corell, J. van Heerden, D. Reinhard, T. Gherezghiher and J. Olivier (2012). "Fog as a fresh-water resource: overview and perspectives." Ambio **41**(3): 221-234.
- Li, B., L. Wang, K. F. Kaseke, L. Li and M. K. Seely (2016). "The impact of rainfall on soil moisture dynamics in a foggy desert." PloS one **11**(10): e0164982.
- Li, B., L. Wang, K. F. Kaseke, R. Vogt, L. Li and M. K. Seely (2018). "The impact of fog on soil moisture dynamics in the Namib Desert." Advances in Water Resources **113**: 23-29.
- Mazaheri, M. R. and M. Mahmoodabadi (2012). "Study on infiltration rate based on primary particle size distribution data in arid and semiarid region soils." Arabian Journal of Geosciences **5**(5): 1039-1046.
- McHugh, T. A., E. M. Morrissey, S. C. Reed, B. A. Hungate and E. Schwartz (2015). "Water from air: an overlooked source of moisture in arid and semiarid regions." Scientific reports **5**: 13767.
- Prada, S., M. M. de Sequeira, C. Figueira and M. O. da Silva (2009). "Fog precipitation and rainfall interception in the natural forests of Madeira Island (Portugal)." Agricultural and Forest Meteorology **149**(6): 1179-1187.
- Saito, H., J. Šimůnek and B. P. Mohanty (2006). "Numerical analysis of coupled water, vapor, and heat transport in the vadose zone." Vadose Zone Journal **5**(2): 784-800.

- Sakai, M., S. B. Jones and M. Tuller (2011). "Numerical evaluation of subsurface soil water evaporation derived from sensible heat balance." Water Resources Research **47**(2).
- Sawaske, S. R. and D. L. Freyberg (2015). "Fog, fog drip, and streamflow in the Santa Cruz Mountains of the California Coast Range." Ecohydrology **8**(4): 695-713.
- Schaap, M. G., F. J. Leij and M. T. Van Genuchten (2001). "Rosetta: A computer program for estimating soil hydraulic parameters with hierarchical pedotransfer functions." Journal of Hydrology **251**(3-4): 163-176.
- Shanyengana, E., J. Henschel, M. Seely and R. Sanderson (2002). "Exploring fog as a supplementary water source in Namibia." Atmospheric Research **64**(1): 251-259.
- Šimůnek, J., M. Šejna, H. Saito, M. Sakai and M. T. Van Genuchten (2013). "The HYDRUS-1D Software Package for Simulating the One-Dimensional Movement of Water." Heat, and Multiple Solutes in Variably-Saturated Media, Version 4: 281.
- Van Genuchten, M. T. (1980). "A closed-form equation for predicting the hydraulic conductivity of unsaturated soils 1." Soil science society of America journal **44**(5): 892-898.
- Wang, L., P. d'Odorico, J. Evans, D. Eldridge, M. McCabe, K. Caylor and E. King (2012). "Dryland ecohydrology and climate change: critical issues and technical advances." Hydrology and Earth System Sciences **16**(8): 2585-2603.
- Wang, L., K. F. Kaseke and M. K. Seely (2017). "Effects of non-rainfall water inputs on ecosystem functions." Wiley Interdisciplinary Reviews: Water **4**(1): e1179.
- Wuest, S. B., S. L. Albrecht and K. W. Skirvin (1999). "Vapor transport vs. seed-soil contact in wheat germination." Agronomy journal **91**(5): 783-787.

Zhang, J., Y.-m. Zhang, A. Downing, J.-h. Cheng, X.-b. Zhou and B.-c. Zhang (2009).

"The influence of biological soil crusts on dew deposition in Gurbantunggut Desert, Northwestern China." Journal of Hydrology **379**(3): 220-228.

CURRICULUM VITAE

Bishwodeep Adhikari

Education

August 2019 Indiana University – Purdue University Indianapolis (IUPUI), USA

Master of Science in Geology

(Advisor: Lixin Wang)

Thesis: The contributions of soil moisture and groundwater to non-rainfall water formation in the Namib Desert

December 2011 Tribhuvan University (TU), Nepal

Bachelor in Civil Engineering

Research and Teaching Experiences

Research Assistant IUPUI Ecohydrology Lab, Department of Earth Sciences, Indianapolis, Indiana (August 2017 – August 2019).

Teaching Assistant Environmental Geology Lab, IUPUI, Department of Earth Sciences, Indianapolis, Indiana (August 2017 – May 2019).

Lecturer Sagarmatha Engineering College, Lalitpur, Nepal (November 2013 – July 2017)

Presentations

- Adhikari, B. and Wang, L. 2018. Groundwater and soil moisture contribution in fog formation and its future in the Namib Desert. Poster. American Geophysical Union (AGU), Fall Meeting, Washington D.C.

- Adhikari, B. and Wang, L. 2018. Groundwater and soil moisture - potential sources of fog in the Namib Desert?. Poster. Geological Society of America (GSA), 130th Annual Meeting, Indianapolis.